

1
2 Extended sialylated O-glycan repertoire of human urinary
3
4
5
6 glycoproteins discovered and characterized using EThcD
7
8
9
10
11

12 *AUTHOR NAMES*

13
14 *Zsuzsanna Darula^{1*}, Ádám Pap^{1,2}, Katalin F. Medzihradszky^{1*}*
15
16
17

18
19 *CORRESPONDING AUTHORS*

20
21 *Zsuzsanna Darula*

22
23 *e-mail: darula.zsuzsanna@brc.mta.hu*
24
25
26
27

28 *Katalin F. Medzihradszky*

29
30 *e-mail: medzihradszky.katalin@brc.mta.hu*
31
32
33
34

35 *ADDRESS*

36
37 ¹Biological Research Centre of the Hungarian Academy of Sciences, Temesvari krt. 62., H-6726 Szeged,
38
39 Hungary
40
41
42
43

44 ²Doctoral School in Biology, Faculty of Science and Informatics, University of Szeged, Közép fasor 52., H-
45
46 6726 Szeged, Hungary
47
48
49
50
51
52
53
54
55
56
57
58
59
60

1 ABSTRACT
2

3
4 A relatively novel activation technique, EThcD was used in the LC-MS/MS analysis of tryptic glycopeptides
5
6 enriched with wheat germ agglutinin from human urine samples. We focused on the characterization of
7
8 mucin-type O-glycopeptides. EThcD in a single spectrum provided information on both the peptide
9
10 modified and the glycan carried. Unexpectedly, glycan oxonium ions indicated the presence of O-acetyl, and
11
12 even O-diacetyl-sialic acids. B and Y fragment ions revealed that i) in core 1 structures the Gal residue
13
14 featured the O-acetyl-sialic acid, when there was only one in the glycan; ii) several glycopeptides featured
15
16 core 1 glycans with disialic acids, in certain instances O-acetylated; iii) the disialic acid was linked to the
17
18 GalNAc residue whatever was the degree of O-acetylation; iv) core 2 isomers with a single O-acetyl-sialic
19
20 acid were chromatographically resolved. Glycan fragmentation also helped to decipher additional core 2
21
22 oligosaccharides: a LacdiNAc-like structure, glycans carrying sialyl Lewis^{X/A} at different stages of O-
23
24 acetylation, and blood antigens. A sialo core 3 structure was also identified. We believe this is the first study
25
26 when such structures were characterized from a very complex mixture and were linked not only to a specific
27
28 protein, but also the sites of modifications have been determined.
29
30
31
32

33
34
35
36 KEYWORDS

37
38 affinity chromatography, blood-type antigen, disialic acid, EThcD, mass spectrometry, O-acetyl-sialic acid,
39
40 O-glycopeptides, urinary glycoproteins, wheat germ agglutinin
41
42
43
44
45
46
47
48
49
50
51
52
53
54
55
56
57
58
59
60

1 INTRODUCTION

2
3
4 Protein glycosylation is a common post-translational modification that is responsible for a wide range of
5
6 biochemical interactions. Protein glycosylation can be C-, N-, O- and S-linked and hence a range of amino
7
8 acid side-chains harbor these glycan linkages¹. O-glycosylation may alter Ser and Thr side-chains within the
9
10 cytosol as well as within the Golgi^{1,2}. While the intracellular proteins feature a single GlcNAc as
11
12 modification, the Golgi-derived glycans are much more complex, with alternate cores that are usually
13
14 elongated^{1,2}. In mammals the GalNAc-core (mucin-type) glycosylation is the most common^{1,2}. Mucin-type
15
16 O-glycosylation of Tyr residues has also been reported recently³. Early on it has also been observed that the
17
18 same sequence positions may or may not be always glycosylated (macroheterogeneity) and may feature
19
20 several different glycans (microheterogeneity)¹. For technical reasons glycoprotein decorating glycans are
21
22 frequently studied after being released⁴⁻⁷. This permits the fractionation and in-depth characterization of
23
24 these oligosaccharides, however, the site-specific information is lost in the process. With the advent of very
25
26 sensitive, high resolution mass spectrometers and new activation techniques, such as ETD (electron transfer
27
28 dissociation⁸) and EThcD (electron-transfer/higher-energy collision dissociation⁹), the focus is shifting
29
30 towards intact glycopeptide or even intact glycoprotein (or at least middle-down) analysis¹⁰. While mass
31
32 spectrometry is suitable for identifying most PTM-bearing sequences in an unbiased manner, collision-
33
34 induced dissociation (CID), the most commonly used MS/MS activation method for obtaining structural
35
36 information on peptides, performs poorly for O-glycopeptide characterization. The culprit is the glycosidic
37
38 bond that is more prone to fragmentation than the peptide bond and thus, fragment ions resulting from sugar
39
40 cleavages dominate the spectra. The glycan is usually completely released from the peptide, without leaving
41
42 any clue behind on the originally modified amino acid. As a result, little to no information is available to
43
44 assign the glycosylation site(s).¹⁰ Hence ion trap CID, i.e. resonance activation only delivers information
45
46 about the glycan size and composition, and the peptide size, while beam-type CID (HCD) may produce
47
48 peptide sequence information, but information on the glycan(s) may be more limited than in ion trap CID
49
50 because of its extensive fragmentation¹⁰. Electron transfer dissociation usually results solely in the peptide
51
52 backbone fragmentation, thus, both the modified amino acid sequence and the modification site(s) can be
53
54
55
56
57
58
59
60

1 assigned⁸. However, ETD spectra frequently yield incomplete sequence ion series, and thus, limited
2
3 information about the glycans present (i.e. it cannot be decided whether the glycopeptide features two small
4
5 glycans or a larger oligosaccharide of the same combined sugar composition) and their location is
6
7 available¹⁰. In the newest activation method, EThcD, electron-transfer is performed first, then newly
8
9 generated fragments and intact precursor ions (activated) are subjected to beam-type collisional activation⁹.
10
11 In this process only some of the ETD-generated fragments undergo further breakdown (such as w ion
12
13 formation¹¹), but the precursor ions are definitely cleaved⁹. Most of this fragmentation results from
14
15 glycosidic bond cleavages, however, the activation is gentler than in normal HCD and the resulting glycan
16
17 fragments are more abundant, while larger structures also survive¹². Thus, we gain information both about
18
19 the peptides modified and the oligosaccharides featured.
20
21
22
23

24 In this manuscript we demonstrate that the information content of EThcD spectra enabled the
25
26 characterization of unexpected/unusual sialylated structures on intact glycopeptides that were enriched from
27
28 the urine of healthy individuals. As far as we know this is the first time that such structures have been
29
30 identified from a complex biological matrix, in a high throughput manner, with protein site specificity. The
31
32 presented method opens new possibilities for the discovery of novel glycan structures with site specificity on
33
34 proteins to reveal their biological function and potential as diagnostic biomarkers.
35
36
37
38
39
40
41
42
43
44
45
46
47
48
49
50
51
52
53
54
55
56
57
58
59
60

1 EXPERIMENTAL
2

3
4 Here we utilized a glycopeptide enrichment strategy as previously described¹². We would like to emphasize
5
6 that no acetate buffer or acetic acid containing solution was used in any part of the protocol. Briefly, tryptic
7
8 digests of urine of 4 healthy donors (collected with appropriate consents approved by the Hungarian
9
10 Scientific and Research Ethics Committee (approval number: 1011/16)) were subjected to a 2-round
11
12 glycopeptide enrichment using a wheat germ agglutinin affinity column collecting 2 glycopeptide fractions
13
14 representing the shoulder of the flow through peak and a fraction eluted by GlcNAc. Fractions were
15
16 analyzed separately by LC-MS/MS using a Waters M-Class nanoUPLC on-line coupled to an Orbitrap
17
18 Fusion Lumos mass spectrometer operated in positive ion mode. Peptides loaded onto a trap column (Waters
19
20 Acquity UPLC MClass Symmetry C18 180 $\mu\text{m} \times 20$ mm column, 5- μm particle size, 100- \AA pore size; flow
21
22 rate 10 $\mu\text{l}/\text{min}$) were separated by a linear gradient of 10-30% B in 60 min (Waters Acquity UPLC M-Class
23
24 BEH C18 75 $\mu\text{m} \times 250$ mm column, 1.7- μm particle size, 130- \AA pore size; solvent A: 0.1% formic
25
26 acid/water; solvent B: 0.1% formic acid/ACN; flow rate: 300 nl/ min), MS/MS data were acquired using
27
28 HCD product-ion dependent EThcD data acquisition mode. The HexNAc-specific oxonium ion, m/z
29
30 204.0867 among the 20 most abundant HCD fragments triggered EThcD acquisition. HCD spectra were
31
32 acquired at 28% NCE, while supplemental activation in EThcD was set at 15% NCE. Precursors with z=3-5
33
34 were considered (intensity threshold: 10^6) according to a decision tree with decreasing charge state and
35
36 increasing precursor m/z, in a total cycle time of 3 s. Some samples were also analyzed using direct injection
37
38 (i. e. without trapping) and allowing z=2 precursors. All measurements were performed in the Orbitrap,
39
40 with a resolution of 60000 and 15000 for MS1 and MS/MS, respectively.

41
42 Separate HCD and EThcD peaklists were generated using Proteome Discoverer (Thermo Scientific,
43
44 v2.2.0.388) requiring at least 40 peaks per spectrum. EThcD data were filtered for the presence of m/z
45
46 292.0927 within the top 20 most abundant fragment ions (required mass accuracy: 10 ppm) using the MS-
47
48 Filter software of Protein Prospector¹³ and retained spectra were searched using the Protein Prospector
49
50 search engine with the following settings: enzyme: semitrypsin with maximum 1 missed cleavage site;
51
52 database: human subset of the Swissprot database (2017.9.19.version, 20219 sequences) concatenated with
53
54
55
56
57
58
59
60

1 the same number of random sequences; mass accuracy: 5 ppm for precursor ions, 10 ppm for fragment ions;
2
3 fixed modification: carbamidomethylation (Cys), variable modifications: acetylation (protein N-terminus),
4
5 cyclization (N-terminal Gln), oxidation (Met), and a set of 28 glycan structures representing core 1 and
6
7 core 2 O-glycans with up to 4 sialic acids/glycan (Supporting Information 1, Table S-1) on Ser/Thr. All
8
9 variable modifications were defined as “common” allowing 2 variable modifications per peptide. The 80
10
11 most abundant peaks were considered from each MS/MS spectrum. Glycopeptide identifications were
12
13 accepted applying 5% and 1% FDR on the protein- and peptide-level, respectively, and setting a SLIP-
14
15 score¹⁴ threshold of 6. All identifications presented were validated manually.

16
17
18
19 The raw data files have been uploaded to MassIVE

20
21
22 (<https://massive.ucsd.edu/ProteoSAFe/static/massive.jsp>), the project’s identifier is MSV000083070.

23 24 25 RESULTS

26 27 *The workflow*

28
29 We intend to gain information on the site-specific O-glycosylation of human proteins, and for this purpose
30
31 the analysis of intact glycopeptides from different sources is necessary. In this study tryptic glycopeptides
32
33 were enriched from urine of healthy donors. Previous studies on urinary glycoproteins, applying the sialic
34
35 acid release and capture method¹⁵ or the glycoblotting-assisted O-glycomics approach^{16,17} indicated that core
36
37 2 and disialylated core 1 O-glycans are present at considerable amounts. As glycopeptides bearing these
38
39 structures would not be enriched by lectins frequently used for O-glycopeptide analysis including Jacalin
40
41 and peanut agglutinin, we used wheat germ agglutinin (WGA) that binds a wide array of glycan structures¹⁸⁻
42
43 ²⁰ including both N- and O-glycopeptides. The glycopeptide mixtures were analyzed applying HCD product
44
45 ion-dependent EThcD with mild supplemental activation (15% NCE), and EThcD data were interpreted
46
47 using Protein Prospector¹². As deduced from the number of MS/MS spectra acquired, the two-round lectin
48
49 enrichment was highly efficient: $\geq 94\%$ of the acquired HCD spectra featured the diagnostic glycan
50
51 oxonium ion m/z 204 in all collected WGA fractions¹². N- and O-glycopeptides were identified in separate
52
53 searches (for details see ¹² and Online Resources 3-4 therein). As the vast majority of the glycopeptides
54
55 represented sialylated glycans¹² we used peak lists filtered for the presence of the diagnostic m/z 292. For O-
56
57
58
59
60

glycopeptide identification a-, mono- and disialo core 1 and the disialo core 2 O-glycan structures were considered. Approximately 2/3 of the O-glycosylated sequences reported earlier for urinary proteins¹⁵ were identified along with several new, mostly multiply glycosylated peptides indicating that WGA affords efficient enrichment of O-glycopeptides. However, the overall identification rate was rather low (~5%)¹². One of the obvious reasons is that in order to keep false discovery rates at acceptable levels, only 2 variable modifications per peptide was permitted in these searches. Thus, multiply modified peptides could be (mis)assigned only if the combined sugar composition of their glycans equaled to a permitted combination. Obviously, glycopeptides with glycans other than the specified structures were also missed.

Iterative search for unexpected/unusual structures

In order to learn what additional structures occur on the glycopeptides enriched, a non-specified modification search^{18,19} was performed on proteins whose presence was already ascertained: any modification up to 3000 Da was allowed on Asn, Ser and Thr residues. From the recurring modification masses and manual inspection of some corresponding MS/MS spectra we concluded that structures containing disialic acids or O,N-diacetylneuraminic acid(s) also were present and needed to be considered. Thus, a more complete glycan database was designed (Table S-1) and a new database search was performed with these accurately defined structures as variable modifications. Then the assigned spectra were carefully inspected. We observed earlier with O-glycopeptides bearing sialyl core 1 and core 2 structures, that the mild supplemental activation during EThcD enables the detection of higher-mass oxonium ions, sometimes even the intact glycan¹². We hypothesized that such ions together with Y-type fragments (for nomenclature see ²¹) could be used to decipher the glycan structures, for example, the linkage position of the unusual disialic acid moiety and the O,N-diacetylneuraminic acids. In addition, our observations could be used to establish fragmentation rules for the identification of novel structures.

The final list of unexpected sialic acid-containing glycoforms derived from the above searches is presented in Table 1. Table S-2 and Figures S-1-29 contain additional information about the identifications and display the supporting MS/MS data. As the focus of this manuscript is to demonstrate how EThcD data can be used for glycan structure elucidation, only fragmentation relevant to the glycan structures is detailed below

(although we would like to point out that peptide side-chain w ions were observed in several spectra that may aid peptide identification). Here we would like to emphasize that our data does not distinguish the isomeric sugar units, resolve position or the stereochemistry of the glycan linkages. These assignments (if presented) are based on assumptions and on our general knowledge on mucin-type glycosylation. However, as described below, the MS/MS spectra usually provided sufficient information on the direct connection of the sugar units or on the branching of the glycans.

Table 1. Glycopeptides carrying O-glycans with O-acetyl- and/or disialic acid(s)¹

Uniprot Acc #	Protein Name	Peptide ²	Tetra ³		Penta ³			Hexa ³		
			1	2	0	1	2	3	1	2
Q9GZM5	Protein YIPF3	³⁴² AVAV T LQSH ³⁵⁰	+	+	+	+	+	+	+	+
P01344	Insulin-like growth factor II	⁹³ DVSTP T VLPDNFPR ¹⁰⁷			+	+				
P78423	Fractalkine	¹⁷⁵ AQDGGPVG T ELF ¹⁸⁶				+				
		¹⁷⁵ AQDGGPVG T ELFR ¹⁸⁷				+				
		²⁴⁷ VWGQGQ S PRPE ²⁵⁷				+				
		²⁴⁷ VWGQGQ S PRPENSLER ²⁶²			+	+				
		²⁶³ EEMGPVPAH T DAF ²⁷⁵			+	+				
Q9BZL3	Small integral membrane protein 3	¹ MDAV S QVPMEVVLPK ¹⁵	+			+				
P98160	Basement membrane-specific heparan sulfate proteoglycan core protein	³³ SLPEDIETV T ASQMR ⁴⁷			+					
		⁴⁸ W T HSYL ⁵³				+				
Q13508	Ecto-ADP-ribosyltransferase 3	³¹⁶ ILEP T QIPGMK ³²⁶	+							
Q9H2B2	Synaptotagmin-4	⁹ EEFDEIPT V VGIF ²¹				+				
Q8TBP5	Membrane protein FAM174A	⁵⁰ PR T LPPLPPG T PAQQPGR ⁶⁸	+							
P09603	Macrophage colony-stimulating factor 1	³⁷⁰ VGPVRP T GQDWNHTPQK ³⁸⁶			+					
P14209	CD99 antigen	²⁹ SDALPDNENKK T AIPK ⁴⁵			+					
P60022	Beta-defensin 1	²² GNFL T GLGHR ³¹			+					

¹ identified by Protein Prospector and validated manually.

² Ser/Thr residues printed in red denote the site of glycosylation.

1 ³Tetra, penta and hexa stands for the total number of the monosaccharides within the glycan structure.

2
3
4 Numbers in the next row specify the number of NeuAcAc residues in the glycan. Proposed structures are
5
6 shown in Table S-1, and in Figures S1-29.

7
8
9
10 *EThcD fragmentation 'rules' at low normalized collision energy*

11
12
13 As a general observation, gentle supplemental energy (NCE: 15%) applied in EThcD typically seemed to
14
15 favor single bond cleavages. Glycan fragmentation yielded non-reducing end B ions, frequently even larger
16
17 (up to 6 residues) oligosaccharides were detected¹², and less prominent internal fragments could be observed
18
19 compared to HCD (acquired with NCE: 28%) (Figures S-1-29 display the corresponding HCD and EThcD
20
21 spectra for each assigned glycopeptide, in certain instances we highlighted the fragmentation differences).
22
23 These ions together with reducing end Y fragments usually provided insight into the glycan structure as
24
25 detailed below.

26
27
28
29 *O-acetyl-sialic acid-containing glycans*

30
31 Fragments at m/z 334.113 and 316.103 indicated the presence of 9-O-acetyl,N-acetylneuraminic acid
32
33 (Neu5,9Ac₂ according to convention, but defined as NeuAcAc in the database searches) within some glycan
34
35 structures (m/z 316 represents water-loss from Neu5,9Ac₂). Obviously, from these data it cannot be
36
37 determined which position was acetylated, however, this structure is the most likely¹. Screening for these
38
39 fragments with MS-Filter of Protein Prospector¹³ showed that ~5% of all EThcD spectra featured at least
40
41 one of these oxonium ions. Database searches allowing Neu5,9Ac₂ (NeuAcAc) containing glycans yielded
42
43 confident identifications (Table 1, Table S-2, Figures S-1-29).

44
45
46
47 Neu5,9Ac₂ was always found in terminal position as evidenced by the Y ions formed via Neu5,9Ac₂-loss
48
49 from the charge-reduced precursors. Confidently assigned glycopeptides featured tetra-, penta- and
50
51 hexasaccharides with up to three Neu5,9Ac₂ residues/glycan (Table 1). However, manual evaluation altered
52
53 the assignment that indicated the presence of an 'internal' Neu5,9Ac₂ (see below).

54
55
56 In the core 1 tetrasaccharides containing one Neu5,9Ac₂, this sugar was Gal-linked as evidenced by the B₂
57
58 ion representing GalNeu5,9Ac₂ (at m/z 496.166) and the corresponding Y_{1,α} ion, at m/z 710.345(2+) (Figure
59
60

1) This B₂ ion in EThcD is usually of higher abundance than the GalNAcNeuAc internal fragment (at m/z 495.182) that is more prominent in HCD (see Figure S-1). Actually, the GalNeu5,9Ac₂ B₂ ion may be overlooked in HCD as the isotopic peak of the internal fragment. The ion at m/z 990.34 represents the intact oligosaccharide.

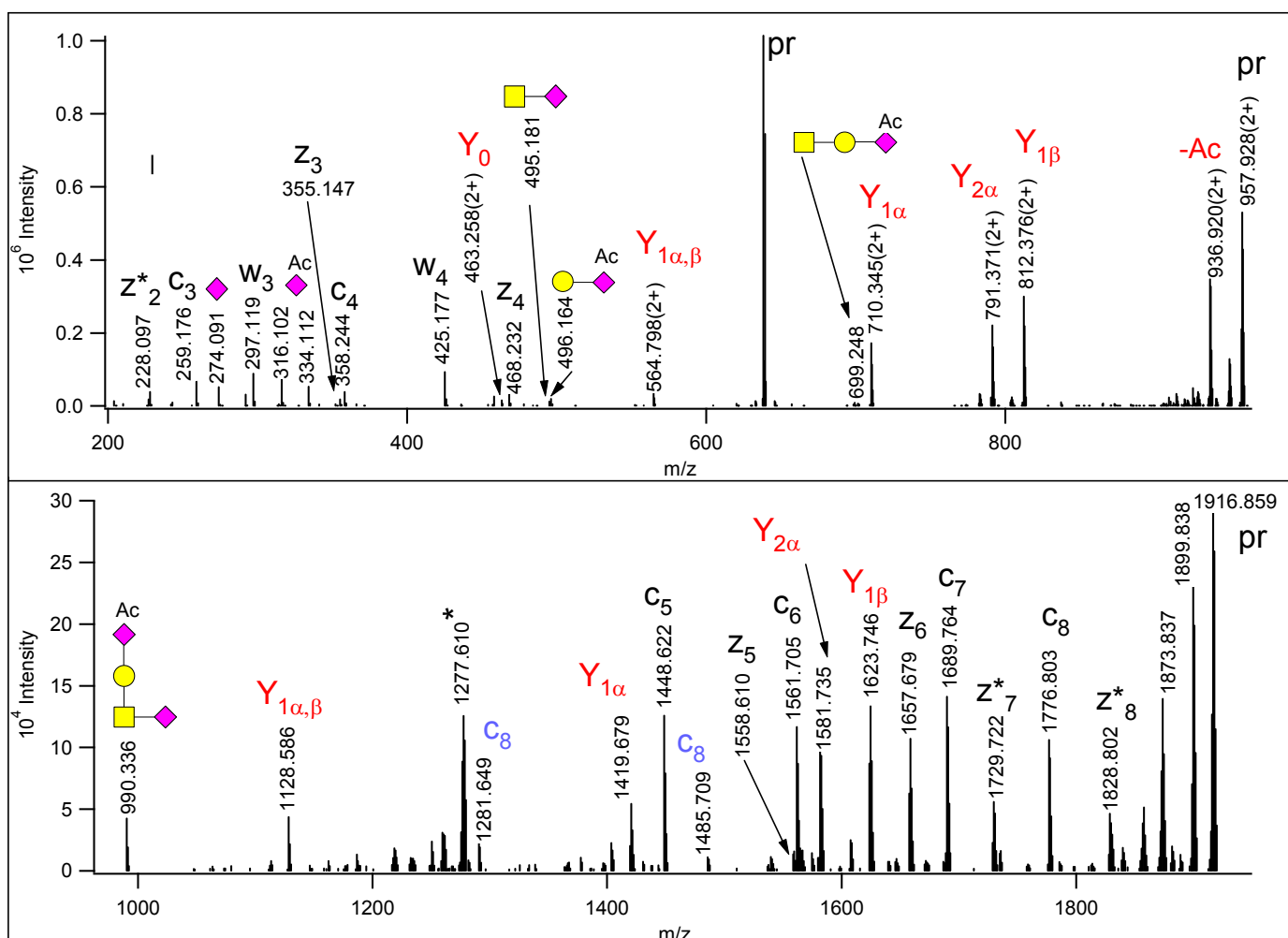


Figure 1. EThcD spectrum of m/z 638.954(3+), identified as

³⁴²AVAVT(HexNAcHexNeuAcNeuAcAc)LQSH³⁵⁰ of Protein YIPF3. The Gal of the mucin-type core 1 structure is capped with a Neu5,9Ac₂ moiety. (This sugar is listed as NeuAcAc in the glycan library for database searches). Oxonium and related ions are labeled according to the CFG recommendations, for the reducing end fragments – printed in red - the Domon-Costello nomenclature is followed²¹. The sialic acid loss from the core GalNAc yields the Y_{1β} fragment. z+1 peptide ions are distinguished with asterisks. Peptide fragments in blue indicate that some glycan fragmentation occurred in EThcD, the loss of the

1 NeuAc and GalNeu5,9Ac₂ from the c₈ fragment, respectively. The asterisk-labeled ion is the charge-reduced
2 form of a doubly charged coeluting molecule.
3
4

5
6
7 In a disialo core 2 hexasaccharide with one Neu5,9Ac₂, this capping residue can be linked to either of the
8 galactoses. Protein Prospector delivered the same identification for EThcD data acquired at different time
9 points from precursor ion m/z 760.664(3+), as ³⁴²AVAVT(HexNAc₂Hex₂NeuAcNeuAcAc)LQSH²⁵⁰ of
10 Protein YIPF3 (Q9GZM5) (Figures S-7 & S-8). Both spectra display the intact glycan fragment (at m/z
11 1355.46) to confirm the presence of a hexasaccharide as opposed to two smaller structures, and Neu5,9Ac₂
12 is Gal-linked (see m/z 496.166). However, as Figure 2 shows in detail, two isomeric glycoforms were
13 present in this sample. In the earlier eluting, more abundant glycoform, the Neu5,9Ac₂ is capping the
14 GlcNAc-Gal arm (designated as 'β-chain', Figure 2, lower panel). This arm can readily be removed by a
15 single cleavage yielding an oxonium ion of HexNAcHexNeuAcAc composition at m/z 699.245 (B_{3β}), and
16 the corresponding Y_{1β} fragment at m/z 791.372(2+). These ions are missing from the other isoform, where
17 the Neu5,9Ac₂ is capping the core GalNAc-linked Gal (designated as 'α-chain', Figure 2, upper panel).
18 Thus, when the bond between the core GalNAc and its modifying GlcNAc is cleaved, an abundant B_{3β} can
19 be observed at m/z 657.234, and the corresponding Y_{1β} was recorded at m/z 812.378(2+). The other
20 fragments are of identical composition, but they are the products of different bond cleavages as indicated in
21 their assignments. In addition, the relative intensities of Y_{1α} and Y_{2β} are different, it seems that the cleavage
22 between the core GalNAc and Gal is preferred to that between the GlcNAc and the Gal linked to it. Here
23 again, we would like to point out that the internal fragmentation of the glycan is less extensive than in HCD:
24 m/z 366.139 representing HexNAcHex is more abundant in the HCD spectra, and the HexNAc₂ fragment
25 (m/z 407.166) was not detected in EThcD (See Figures S 7-9).
26
27
28
29
30
31
32
33
34
35
36
37
38
39
40
41
42
43
44
45
46
47
48
49
50
51
52
53
54
55
56
57
58
59
60

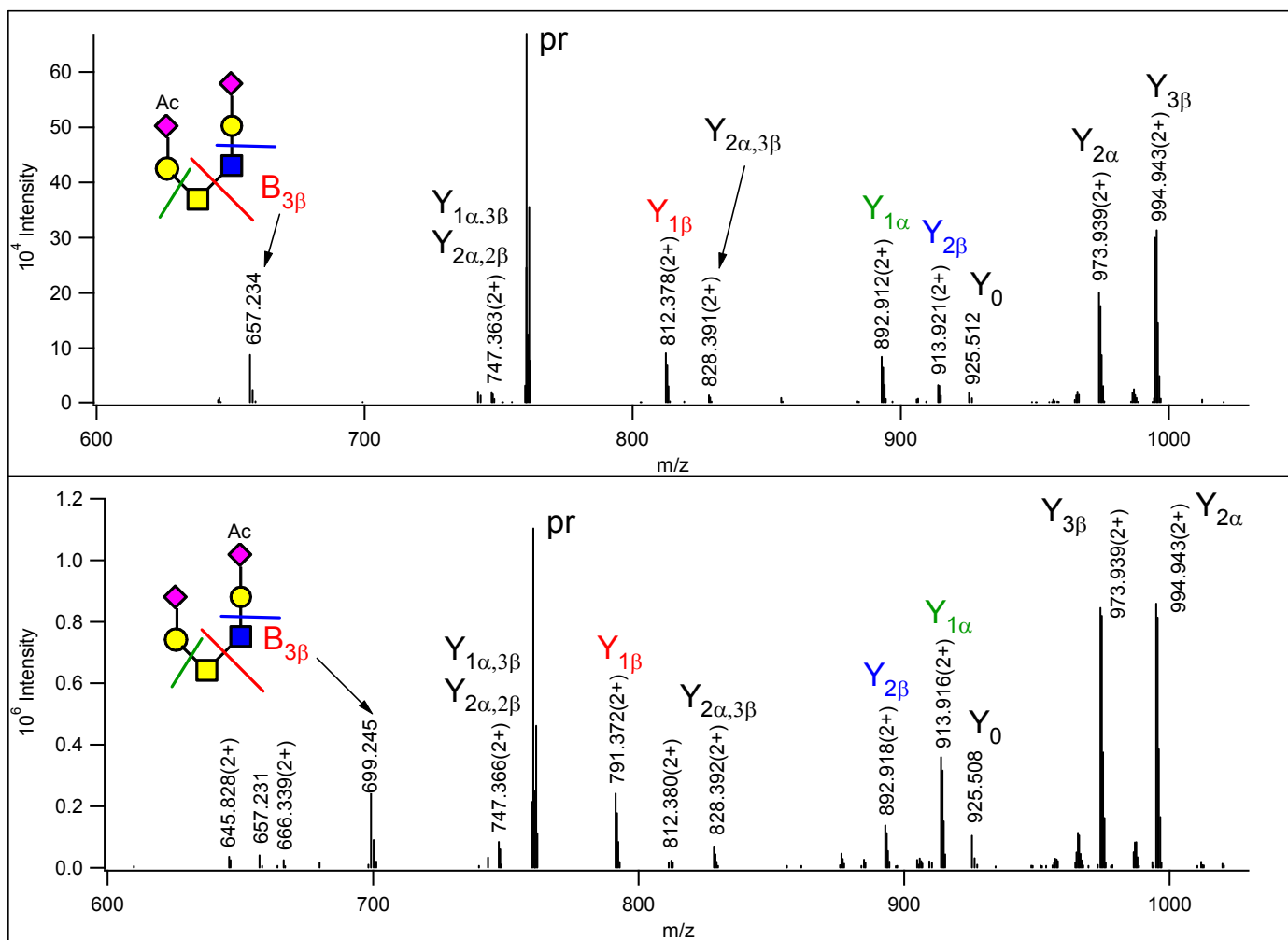


Figure 2. Part of the EThcD spectra acquired from m/z 760.664(3+) at $RT=14.95\text{min}$ (Lower panel) and at $RT=18.29\text{min}$ (Upper panel). Both spectra were assigned as

$^{342}\text{AVAVT}(\text{HexNAc}_2\text{Hex}_2\text{NeuAcNeuAcAc})\text{LQSH}^{350}$ of Protein YIPF3 (for full spectra see Figures S-7 & S-8). (NeuAcAc stands for Neu5,9Ac₂ in the glycan library for database searches.) However, the glycan fragments revealed isomeric glycoforms. The diagnostic fragment ions and the underlying cleavages are indicated in matching colors.

Finally, an identification indicated the presence of a pentasaccharide structure with three NeuAcAc residues (Figure 3). Although the additive mass of the glycan (1364.45 Da) is correct, we found this identification highly unlikely as it suggests the presence of a non-terminal Neu5,9Ac₂ considering the structure of the pentasaccharide glycans (see below). Careful investigation of the EThcD spectra revealed that three different sialic acids modified the core 1 glycan: the Gal is capped with a Neu5,9Ac₂, while the GalNAc is linked directly to a NeuAc that is further elongated with a sialic acid bearing 2 ‘extra’ acetyl groups. This is likely

an O-4,9-diacetyl-N-acetylneuraminic acid¹. The presence of such a neuraminic acid derivative, perhaps Neu4,5,9Ac₃, was confirmed by its proper oxonium ion and the corresponding water-loss fragment at m/z 376.124 and 358.112, respectively (both within 4 ppm of the theoretical m/z values). The GalNeu5,9Ac₂ linkage was validated by Y_{1α} representing the loss of the hexose along with the terminal sialic acid, at m/z 897.899(2+). The GalNAc-linked NeuAcNeu4,5,9Ac₃ structure is supported by the observation of the above described Y_{1α} fragment, and by the consecutive losses of Neu4,5,9Ac₃ and NeuAcNeu4,5,9Ac₃ at m/z 957.924(2+) and 978.931(2+), respectively.

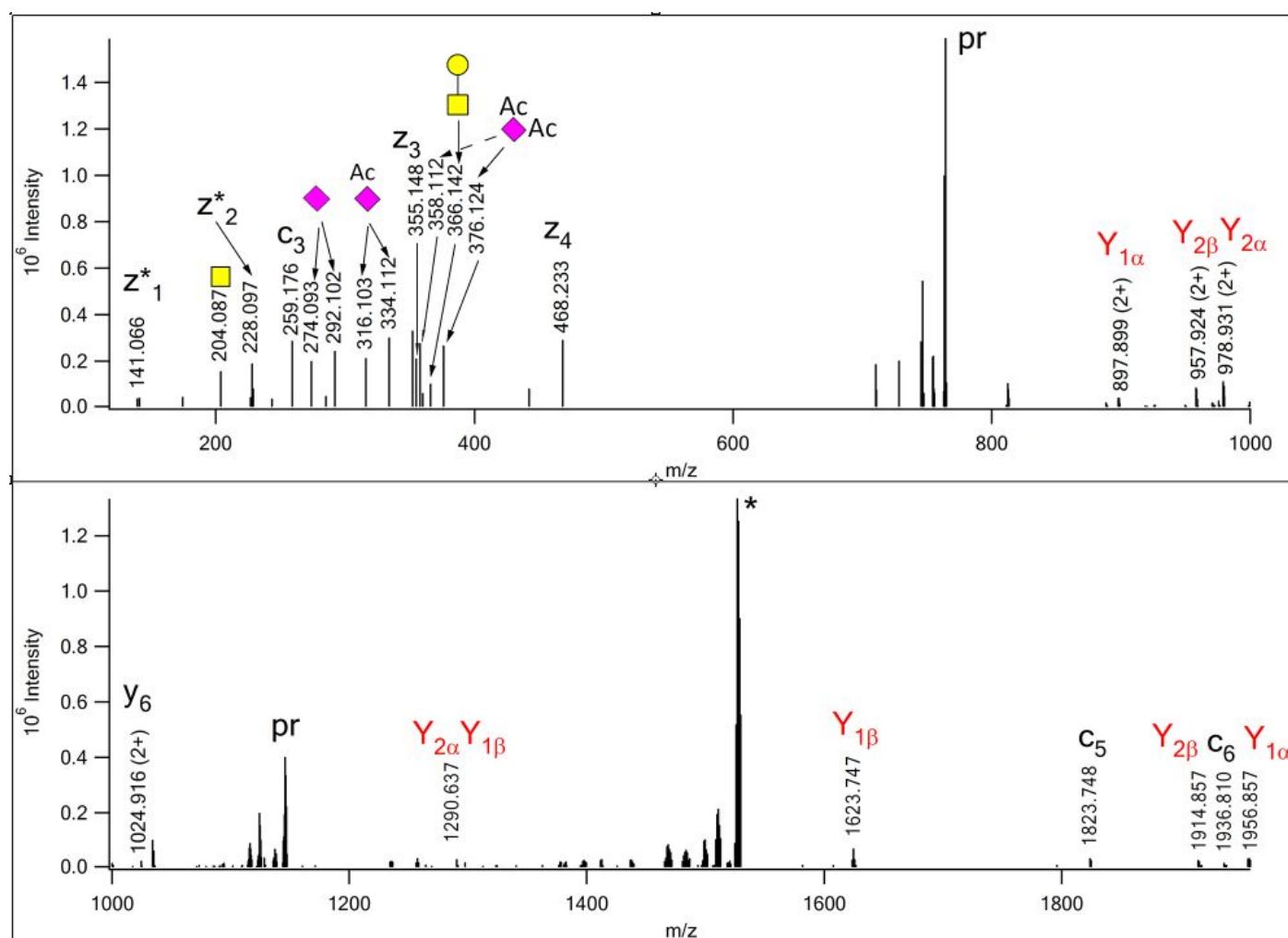
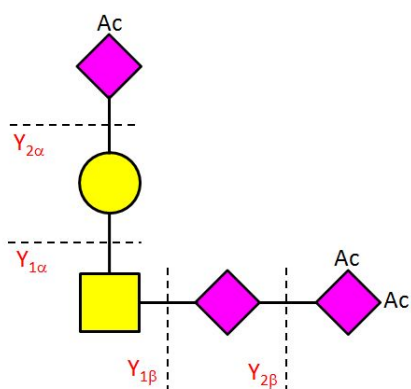


Figure 3. EThcD spectrum of m/z 763.992(3+) manually assigned as ³⁴²AVAVTLQSH³⁵⁰, modified at Thr-346 with a core 1 glycan that features a Neu5,9Ac₂ on the Gal residue, and a NeuAc-Neu4,5,9Ac₃ disialo-unit on the core GalNAc. ‘Pr’ indicates the different forms of the precursor ion. z+1 peptide fragments are distinguished with asterisks. The oxonium ions identifying the three different sialic acids are labeled with the CFG symbols, for the reducing end fragments – printed in red - the Domon-Costello nomenclature is

followed²¹. The GalNAc modifications were considered the β -arm. The asterisk-labeled ion is the charge-reduced form of a doubly charged coeluting molecule.



Scheme 1. Fragmentation of the glycan structure assigned from the spectrum in Figure 3.

Disialic acid-containing glycans

Obviously, there is an overlap between the unusual glycopeptides featuring O-acetyl-sialic acids and the ones bearing core 1 structures modified with a disialic acid unit (Table 1). The terminal residue of this disialic unit may be NeuAc or may bear additional O-acetyl groups, i.e. it may be Neu5,9Ac₂ or Neu4,5,9Ac₃ (as described above). The disialic acid unit usually produces a relatively abundant oxonium ion at m/z 583.197 or 625.210 for (NeuAc)₂ or NeuAcNeu5,9Ac₂, respectively. Filtering for the presence of these ions with MS-Filter¹³ showed that ~2% of all EThcD spectra represented glycopeptides with disialic acid within the glycan structure. The composition of the modifying glycan was frequently confirmed by an oxonium ion representing the intact glycan, at m/z 1239.43 or 1281.44.

EThcD fragmentation of a glycopeptide with a pentasaccharide glycan is illustrated in Figure 4. The glycan carries three “simple” NeuAc units, Y ions representing neutral losses of (NeuAc)₂ at m/z 1156.04(2+), and HexNeuAc at m/z 1220.56(2+) prove that the glycan is branched, and the disialic acid is linked to the core GalNAc. The inter-sialic acid bond is confirmed by the (NeuAc)₂ oxonium ion (B_{2β}) at m/z 583.197. The oxonium ion representing the intact glycan at m/z 1239.41 confirms that a single glycan modifies the peptide. In a similar fashion we could decipher that (whenever there was conclusive evidence) the disialic acid was always GalNAc-linked. Limited internal fragmentation of the glycan was observed for this class of glycopeptides as well. While in HCD the internal fragment representing GalNAcNeuAc (m/z 495.182) was

usually abundant, in EThcD the B₂ ion representing GalNeuAc (m/z 454.155) was dominant (for example, see Figures S-10-12).

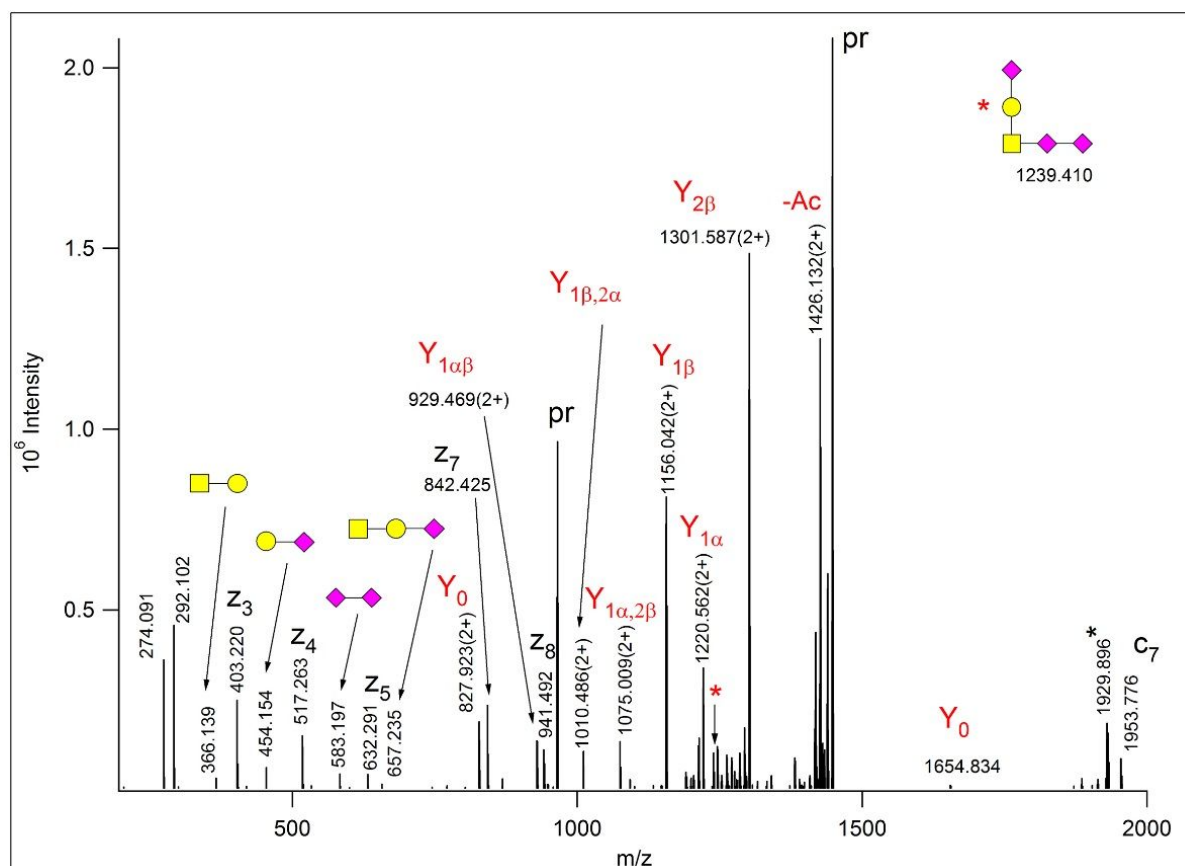


Figure 4. EThcD spectrum of m/z 965.092(3+), identified as

⁹³DVSTPPT(HexNAcHexNeuAc₃)VLPDNFPR¹⁰⁷ of Insulin-like growth factor II. The precursor ion and its charge-reduced form are labeled with ‘pr’. The nonreducing end fragments are labeled with cartoons according to the CFG recommendations, the reducing end fragments, printed in red, follow the nomenclature²¹. The inset shows the intact glycan and its oxonium ion is labeled by a red asterisk. The other asterisk-labeled ion is the charge-reduced form of a doubly charged coeluting molecule. For full peaklist see Figure S-10.

Interestingly, if only one Neu5,9Ac₂ was present in the glycan structure, it was always Gal-linked in the tetrasaccharides, while in pentasaccharides the GalNAc-linked disialic acid was terminated with it.

1 *Additional unusual glycans*

2
3
4 Finally, the database search permitting unspecified modifications delivered two intriguing suggestions. First,
5
6 it identified a glycopeptide with a glycan mass of 1062.39 Da (Figure 5). This mass corresponds to a
7
8 HexNAc₃HexNeuAc glycan composition, that is most unusual for an O-glycan (the calculated mass is
9
10 1062.386, within 2 ppm). The observed non-reducing end B and reducing end Y carbohydrate fragments
11
12 suggest that this unusual glycan might be a Galβ3(GalNAcβ4GlcNAcβ6)GalNAc, the LacdiNAc-like
13
14 structure described by Jin et al.²², from a human gastric mucin sample. We detected this structure modified
15
16 with a sialic acid on the galactose (Figure 5, Scheme 2). More specifically, the fragment ion at m/z 407.165
17
18 confirms the inter-HexNAc linkage and also indicates that this is a terminal HexNAc-HexNAc structure.
19
20 Although m/z 407 can, in principle, also be formed as an internal fragment of core 2 glycans, it was not
21
22 detected in their respective EThcD spectra (see Figures S-7-9). Similarly, m/z 454.154 indicates a terminal
23
24 HexNeuAc group. These ions together with reducing end Y ions unambiguously show that the glycan is
25
26 branched and a HexNeuAc and a HexNAc₂ are linked to the core GalNAc. The B₃ fragment representing the
27
28 intact glycan was detected at m/z 1063.398.
29
30
31
32
33
34
35
36
37
38
39
40
41
42
43
44
45
46
47
48
49
50
51
52
53
54
55
56
57
58
59
60

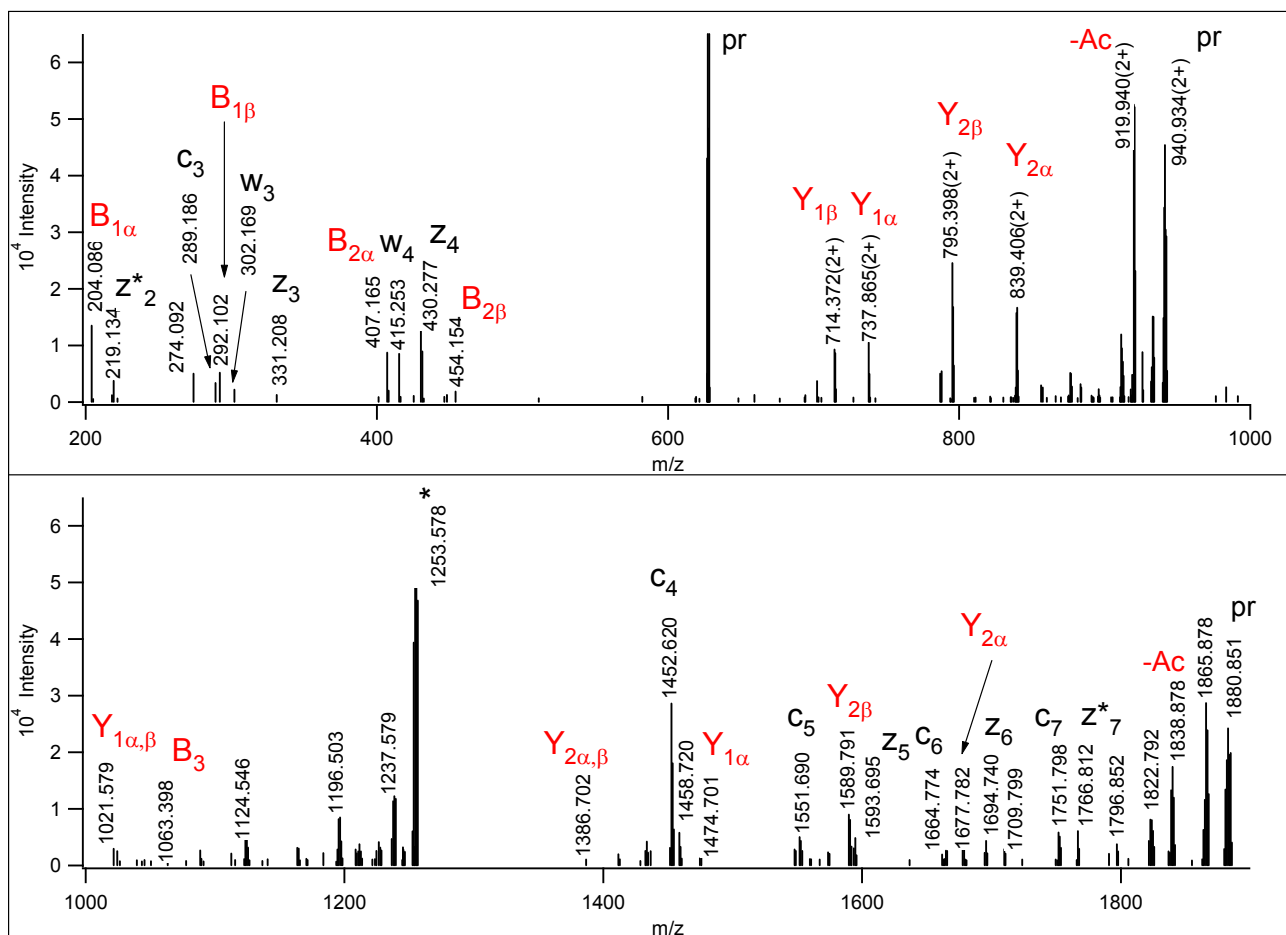
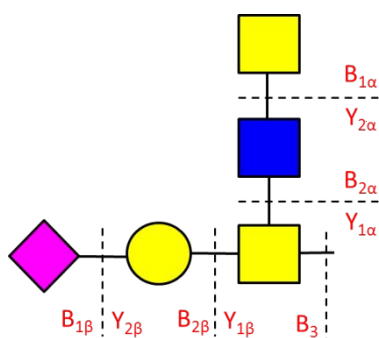


Figure 5. EThcD spectrum of m/z 627.634(3+). The database search permitting unspecified modifications identified as $^{45}\text{VATT}(1062.388)\text{VISK}^{52}$ of Plasma protease C1 inhibitor. z^* indicates a $z+1$ peptide fragment. The intact glycan oxonium ion confirms that the peptide is modified by a single oligosaccharide of HexNAc₃HexNeuAc composition. The glycan fragments helped to decipher the branching and linkages within the oligosaccharide, a core 2 based LacdiNAc-like structure²². Scheme 2 illustrates which bonds are cleaved. z^* indicates a $z+1$ peptide fragment. The asterisk-labeled ion is the charge-reduced form of a doubly charged coeluting molecule.



Scheme 2. Fragmentation of the glycan structure assigned from the spectrum in Figure 5.

1
2
3
4 The second fascinating identification was $^{345}\text{SLTVS}(1370.497)\text{LGPVSKT}(\text{HexNAcHexNeuAc})\text{EGFPK}^{361}$
5
6 from Protein HEG homolog 1 (Q9ULI3), where the modification mass, suggested by the search engine,
7
8 corresponded to a $\text{HexNAc}_3\text{Hex}_2\text{FucNeuAc}$ composition, that could represent a core 2 structure bearing an
9
10 A-type antigen (see later). However, an abundant oxonium ion at m/z 674.252 ($\text{HexNAcHex}_2\text{Fuc}$) and the
11
12 similarly abundant corresponding Y fragment, at m/z 1034.16 (3+) strongly suggested the presence of a core
13
14 2 glycan carrying a blood-type B antigen. The assigned modifications and the fragments observed
15
16 contradicted each other. Our investigation revealed that a series of unassigned doubly charged fragment ions
17
18 could be identified as z ions (z_7 - z_{12}) from the mass differences between them. These fragments' mass shift
19
20 (697 Da) clearly indicated that the Thr carries a $\text{HexNAc}_2\text{NeuAc}$ oligosaccharide, most likely a sialylated
21
22 core 3 structure, i.e. a $\text{GlcNAc}\beta 3(\text{NeuAc}\alpha 6)\text{GalNAc}$ instead of the core 1 trisaccharide. The oxonium ion
23
24 of this glycan was subsequently identified at m/z 698.266. Thus, the 'leftover' glycan on Ser-349 features a
25
26
27
28
29
30
31
32
33
34
35
36
37
38
39
40
41
42
43
44
45
46
47
48
49
50
51
52
53
54
55
56
57
58
59
60
HexNAc₂Hex₃FucNeuAc composition that is indeed a core 2 structure decorated with the B blood-type
antigen (Figure 6, Scheme 3). The donor's blood type was AB.

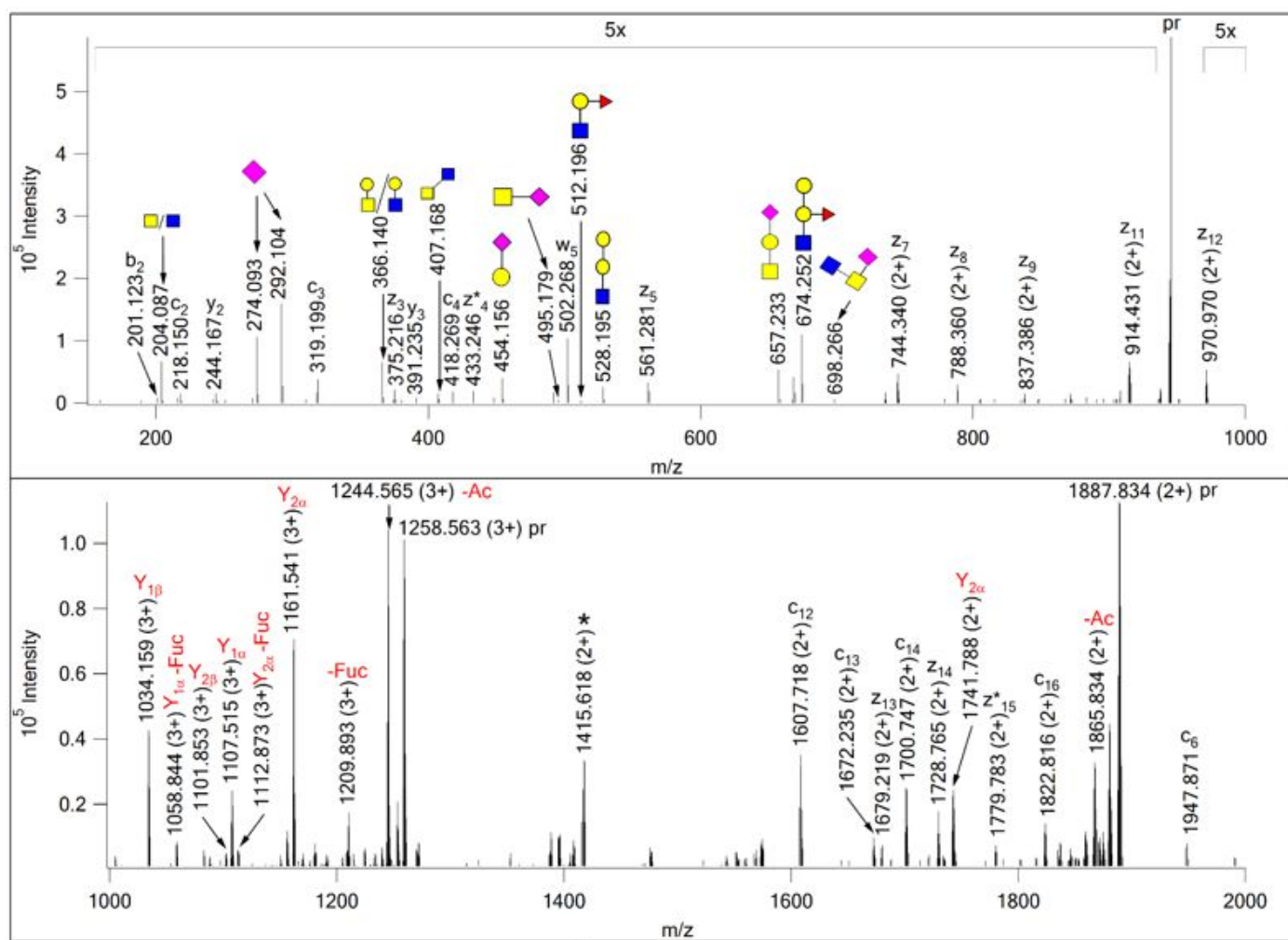
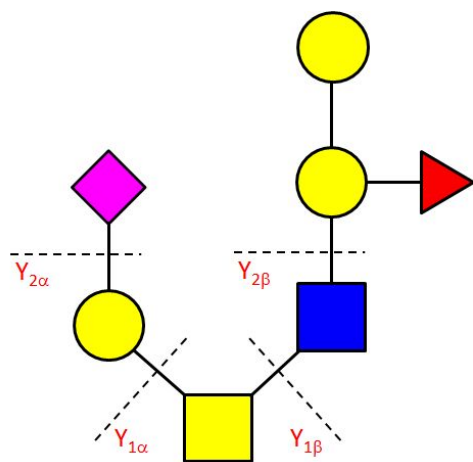


Figure 6. EThcD spectrum of m/z 944.178 (4+) manually assigned as $^{345}\text{SLTVS}^*\text{LGPVSKT}^*\text{EGFPK}^{361}$ from Protein HEG homolog 1 (Q9ULI3), with a core 2 structure carrying a B-antigen on Ser-349 and a sialyl core 3, GlcNAc β 3(NeuAc α 6)GalNAc on Thr-356. The intact sugar oxonium of this glycan was detected at m/z 698.266. Its modification site was determined from the series of doubly charged z_7 - z_{12} fragments. Scheme 3 illustrates bond cleavages within the larger glycan structure. The precursor ion and its charge-reduced form are labeled with 'pr'; the charge-reduced form of a coeluting doubly charged component is indicated with an asterisk. Y ions reflect the fragmentation of the core 2 glycan carrying the B antigen.



Scheme 3. Fragmentation of the mucin core 2 glycan carrying blood-type antigen B structure assigned from the spectrum in Figure 6.

Targeted glycoform identification for a specific peptide

These unusual structures prompted us to further investigate the presence of additional glycoforms for the peptide that already featured the highest microheterogeneity: $^{342}\text{AVAVTLQSH}^{250}$ of Protein YIPF3. Using the MS-filter option of Protein Prospector¹³ with one of the datafiles representing the earlier eluting glycopeptides, we identified all HCD spectra that displayed the gas-phase deglycosylated Y_0 fragment (m/z 925.510) among the 5 most abundant ions and with a mass measurement error below 10 ppm. Then the potential glycan masses were calculated for each such component and 4 new glycan structures emerged with compositions of $\text{HexNAc}_3\text{Hex}_2\text{FucNeuAc}$, $\text{HexNAc}_2\text{Hex}_2\text{FucNeuAc}_2$, $\text{HexNAc}_2\text{Hex}_2\text{FucNeuAcNeuAcAc}$ and $\text{HexNAc}_2\text{Hex}_2\text{Fuc}(\text{NeuAcAc})_2$, represented by incremental monoisotopic masses of 1370.499, 1458.514, 1500.516 and 1542.537 Da, respectively (Table S-3). Placing these numbers as modifications within the sequence, and comparing the MS-product predictions (Protein Prospector) with the EThcD data it became clear that Thr-346 was always the glycosylation site.

The first structure is most likely, a core-2 glycan carrying the A blood antigen as shown in Figure 7, Scheme 4. While the identity of the sugar units and their linkage positions obviously could not be determined from these data, the connections between the units could be deciphered from the EThcD spectrum (Figure 7). An oxonium ion at m/z 512.202 and the corresponding Y fragment indicated a terminal HexNAcHexFuc structure. Other reducing end fragments identified a hexose-linked sialic acid as well as a terminal HexNAc .

1 Since single bond cleavages are preferred in EThcD, the presence of an abundant B-fragment at m/z 657.237
2
3 and its reducing end counterpart at m/z 820.399(2+) suggest that the core GalNAc is modified with a
4
5 HexNAcHexNeuAc structure and the other extension might be the A-antigen because of its composition and
6
7 terminal HexNAc. These conclusions were further strengthened by the Y_{2β,1α} fragment detected in HCD at
8
9 m/z 1437.715 (Figure S-30). This A-antigen featuring peptide was identified from the same donor as the B-
10
11 antigen carrying molecule described above.
12

13
14 The other sugar compositions suggest the presence of Sialyl Lewis^{X/A} in different stages of O-acetylation
15
16 (See Table S-3; Figures S-31-34). The isomeric structures containing one O-acetyl-sialic acid were
17
18 chromatographically resolved, and the earlier eluting isoform carried this modification on the GlcNAc-
19
20 containing arm, just like in the hexasaccharide isomers presented in Figure 2. Interestingly, all fucose-
21
22 containing glycoforms produced a few ions that indicated fucose transfer between the extensions (Figures 6-
23
24 7, Figures S-31-35). Fucose ‘migration’ has been reported in glycan analyses²³ as well as for N-linked
25
26 glycopeptides^{24,25}.
27
28
29
30
31
32
33
34
35
36
37
38
39
40
41
42
43
44
45
46
47
48
49
50
51
52
53
54
55
56
57
58
59
60

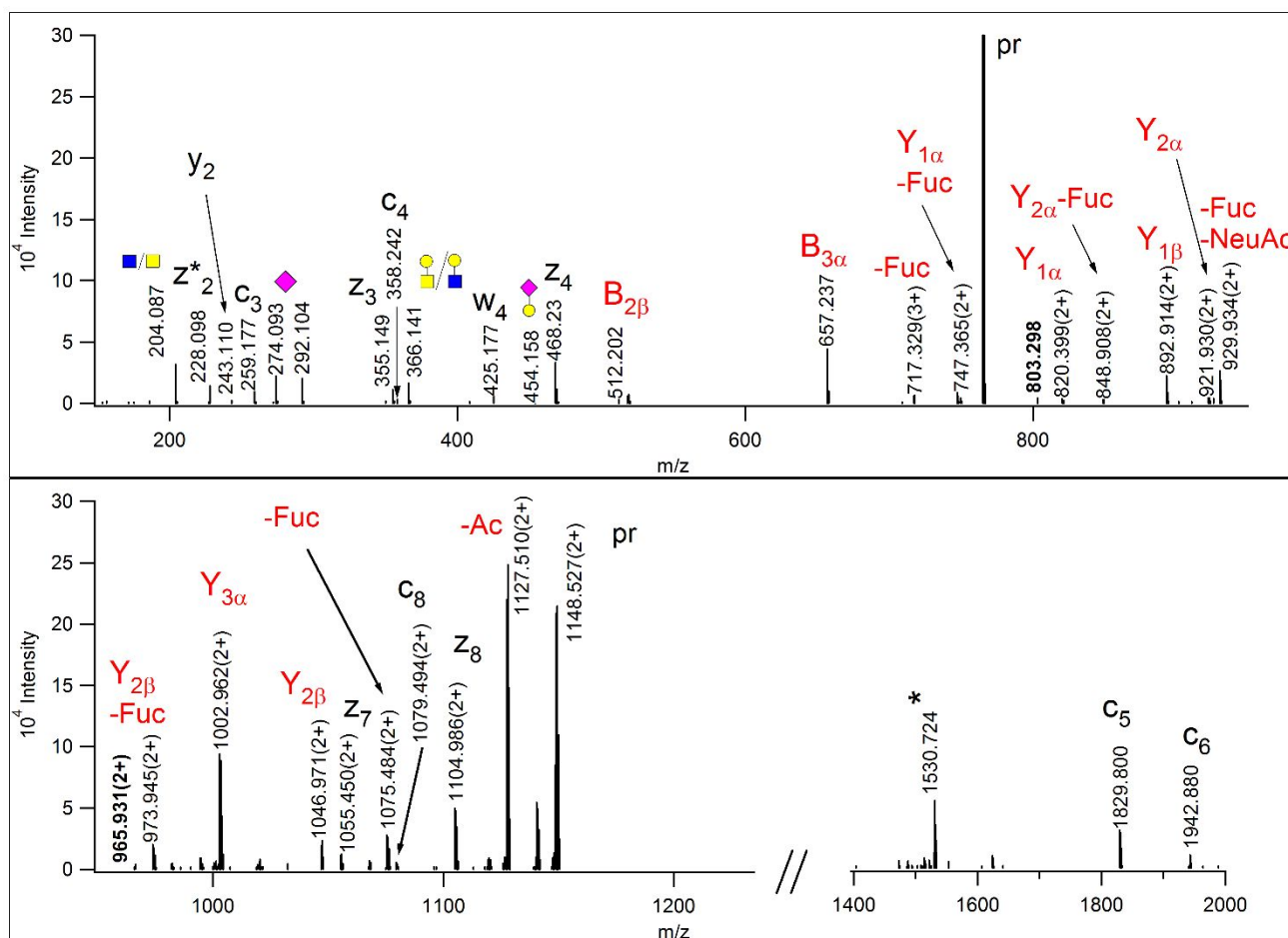
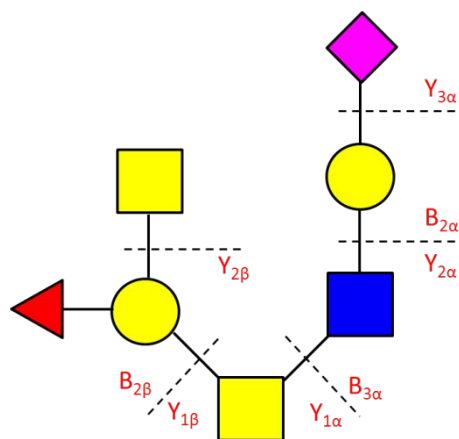


Figure 7. EThcD spectrum of m/z 766.008(3+) that was manually assigned as $^{342}\text{AVAVTLQSH}^{350}$ of Protein YIPF3 bearing a HexNAc₃Hex₂FucNeuAc glycan on Thr-346. The precursor ion and its charge-reduced form are labeled with 'pr'; the charge-reduced form of a coeluting doubly charged component is indicated with an asterisk. The glycan was assigned as a core 2 glycan featuring the A antigen linked to the GalNAc. A similar core 2 A antigen has been described on gastric mucin by Rossez *et al.*²⁶ Scheme 4 illustrates which bonds are cleaved. m/z values printed in bold label fragments that indicate fucose transfer between the antennae: m/z 803.298 represents a HexNAcHexFucNeuAc structure, while m/z 965.931(2+) was formed *via* HexNAcHex loss from the precursor ion.



Scheme 4. Fragmentation of the glycan structure assigned from the spectrum in Figure 7.

In a similar attempt as described above, an additional glycoform of this peptide bearing a more extended sugar structure (HexNAc₃Hex₃FucNeuAc₂, mass increment: 1823.65 Da), representing an extended core 2 glycan decorated with Sialyl Lewis^{X/A} was identified in a later eluting glycopeptide fraction (Figure S-35, Table S-3).

DISCUSSION

In order to understand the biological role(s) of O-glycosylation addressing the site-specificity of the modifications is necessary. However, the enrichment and characterization of O-glycopeptides is an even more daunting task than deciphering N-glycosylation¹⁰.

One tends to believe that mucin-type O-glycosylation operates with only a handful of structures. For example, serum proteins feature primarily mono- and disialo core 1 glycans²⁷. However, the glycan repertoire is much more diverse for gastric mucins^{22,26}, and as presented here the urinary glycoproteome is much more complex as well. Our results also indicate that removing the sialic acids indeed may make the investigated mixtures simpler, but at a significant price i.e. losing valuable information on microheterogeneity. Peptides featuring multiple potential glycosylation sites may display an overwhelming degree of macro- and microheterogeneity. For example, the complexity generated by macroheterogeneity could be illustrated by the glycoforms reported for the ¹⁵⁴Ser-Lys¹⁷⁵ region of bovine insulin-like growth factor II²⁸, while for microheterogeneity we have just presented the ³⁴²Ala-His³⁵⁰ stretch of Protein YIPF3 (its 'normal' disialo core 1, and core 2 glycoforms were described in our earlier report¹²). Obviously, this

1 heterogeneity makes the chromatographic separation of the different glycoforms harder, and may also
2 prevent the detection of minor components. Differentiation between the isomeric structures as well as
3 positional isomers presents an even greater challenge.
4
5
6

7
8 As briefly summarized in the introduction, the different MS/MS activation techniques deliver different clues
9 to solve the glycopeptide puzzle. Unfortunately, these data are rarely used in concert, and primarily via
10 manual data interpretation. Perhaps eventually a software tool will be developed that can utilize orthogonal
11 data sources, but until then EThcD, yielding both glycan and peptide fragments is the best approach for
12 identification. For example, abundant oxonium ions indicate the presence of the different neuraminic acids.
13 The diagnostic value of such Neu5,9Ac₂ fragments has been reported for beam-type CID data¹³, here similar
14 ions revealed the presence of a Neu4,5,9Ac₃ moiety. Oxonium ions of sialic acids are very abundant in the
15 EThcD spectra¹², and in complex mixtures numerous spectra may display them due to precursor ion
16 interference. Thus, they have to be considered with caution as unambiguous evidence for sialylation.
17 However, the lack of these diagnostic oxonium ions clearly signals that no glycan featuring the
18 corresponding sialic acid might be present. Thus, screening the peaklists for such diagnostic fragments
19 could be recommended prior to database searches, or PSMs assigned to sialic acid-containing structures
20 should be considered false whenever the diagnostic oxonium ions were not observed.
21
22
23
24
25
26
27
28
29
30
31
32
33
34
35
36
37

38 In an earlier publication beam-type CID (HCD) spectra of murine nucleobindin-1 glycopeptides illustrated
39 that internal glycan fragments representing the core GalNAc modified with N-acetyl, N-glycolyl, or N,O-
40 diacetylneuraminic acid helped assign the different versions of the disialo-core 1 tetrasaccharides¹³. The
41 HCD data acquired in this study (Figures S-1-35) are in good agreement with these observations. However,
42 while the internal oxonium ion is the dominant species in HCD, the terminal B₂ fragment produced by a
43 single bond cleavage is significantly more abundant in the EThcD spectra. With the mild EThcD activation
44 the products of single bond cleavages are detected preferentially, even if internal fragments may be
45 observed. As described, the glycan fragments help to determine the direct linkages between the sugar units.
46 In fact, the occurrence of B₂ ions representing disialic acids is so high that they might be used as reporter
47 ions for the presence of these disaccharide units, and can be used for prefiltering the peaklists when
48
49
50
51
52
53
54
55
56
57
58
59
60

1 searching for glycopeptides bearing such glycans. While most such glycoforms will be identified in general
2 database searches as well, the FDR rate is higher, and thus, lower scoring true identifications may 'sink' into
3 the background¹². Obviously, these fragments also should be considered as strong evidence in glycopeptide
4 fragmentation scoring. Glycan fragmentation in EThcD also may permit the correct assignment of isomeric
5 structures as presented in this manuscript. It would be beneficial if these observations were incorporated into
6 the automated evaluation of glycopeptide EThcD spectra. The gentler activation also enables, not
7 infrequently, the survival of the oxonium ions representing even penta- or hexasaccharides. The presence of
8 these fragments can help to differentiate between the different glycans or glycan combinations that represent
9 identical mass additions. As these fragment ions are often rather weak, it is not very likely that precursor ion
10 interference could 'inject' them into the spectra. Considering them as positive evidence for the presence of
11 larger glycans is recommended.

12 Manual investigation of the spectra also drew our attention to a peak picking issue. Here we do not refer to
13 the misidentification of the monoisotopic mass in the precursor ion cluster – although this is still a persistent
14 problem. When evaluating the raw spectra there were often additional peaks that could provide glycan
15 structural or site localization information but were not considered by the search engine. Some of these were
16 due to incorrect determination of a fragment monoisotopic peak or removal of a peak during deisotoping,
17 and others were removed by an intensity-based filter. This is likely a result of search engines being
18 optimized for peptide identification; as adding in lower intensity peaks, several of which are background
19 ions, can reduce statistical significance of the peptide assignment.

20 As for the biological significance of our findings, presently we cannot offer any convincing hypothesis.
21 Polysialic acid has been found both in N- and O-glycans, and depending on the degree of polymerization can
22 be categorized as di-, oligo- and polysialic acids²⁹. The presence of such structures is usually determined
23 using immunochemistry. While polysialylation clearly has a role in neural development³⁰, it has also been
24 implied in cancer metastasis³¹. On the other hand, although disialic acid units have been detected on multiple
25 glycoproteins³²⁻³⁶, no clear biological role has been linked to this structure yet. The proteins identified in the
26 present report also participate in diverse biological processes including cell adhesion (Macrophage colony-

1 stimulating factor 1, fractalkine, CD 99), glucose metabolism (insulin like growth factor II) or maintaining
2 the structure of the cell membrane (basement membrane-specific heparan sulfate proteoglycan core protein)
3 or the Golgi (YIPF3).
4
5

6
7
8 Nonetheless, the sialyltransferases catalyzing the formation of disialic acids are known. ST8Sia VI is
9 responsible for disialic acid formation in O-glycans catalyzing the formation of both
10 NeuAc α 2,8NeuAc α 2,3Gal and NeuAc α 2,8NeuAc α 2,6GalNAc structures^{37,38} with higher preference
11 towards the NeuAc α 2,6GalNAc substrate. Our findings are in good agreement with the above observation,
12 disialic acid was linked to the core GalNAc in the glycopeptides characterized. In addition, ST8Sia VI is
13 expressed at higher levels in kidney³⁷, thus, perhaps urinary proteins may feature more of these structures.
14
15 As far as we know this is the only report where site-specific information was obtained on multiple proteins
16 for the disialic acid carrying O-glycopeptides. The only other study describing a similar pentasaccharide
17 structure was reporting on amyloid peptides isolated from human cerebrospinal fluid. However, in that case
18 the pentasaccharide modified a Tyr residue, and MS/MS data indicated that the disialic acid unit was linked
19 to the galactose³.
20
21

22
23 O-acetylation of sialic acid plays a role in cell-cell interactions and non-immune protection of mucosa³⁹. It
24 was suggested that O-acetylation of neuraminic acids on cell surfaces “may protect against pathogen
25 infection by preventing degradation of membrane-associated mucins”⁴⁰. At the same time another report
26 links the expression of O-acetyl sialoglycoproteins on erythrocytes to leukemia⁴¹. None of these studies
27 characterized the O-acetylneuraminic acid-containing glycan structures, or pinpointed their location within
28 any particular protein or residue.
29
30

31
32 Finally, the presence of blood-type antigens has been documented on gastric mucins²⁶, but as far as we are
33 aware this is the first time that a glycopeptide is presented bearing such a structure.
34
35

36 CONCLUSION

37
38 We demonstrated that EThcD with gentle supplemental activation (NCE 15%) may deliver quite
39 comprehensive information for O-glycopeptide structure elucidation. In this process we extended the
40 sialoglycan repertoire of urinary glycoproteins. We unambiguously established the presence of a variety of,
41
42
43
44
45
46
47
48
49
50
51
52
53
54
55
56
57
58
59
60

1 never reported, mucin-type structures with O-acetyl-sialic acid(s), disialic acids or both. In addition, we also
2
3 identified a trisialo core 1 glycan with O-diacetylsialic acid, and characterized a series of unusual core-2
4
5 structures, including ones displaying a blood-type antigen.
6
7

8 We observed that the detected glycan oxonium ions were mostly B fragments, and the Y fragments also
9
10 indicated some preference for single bond cleavages. We identified some diagnostic oxonium ions that may
11
12 not unambiguously prove the presence of certain structures because of the precursor ion interference in such
13
14 complex mixtures, but their absence is determinative. Larger fragments representing intact penta- and
15
16 hexasaccharides were also detected. We believe these should be more positively considered during scoring.
17
18 These observations should lead to improved automated glycopeptide assignments using EThcD data and the
19
20 resulting methods will provide tools aimed at elucidating this complex yet understudied class of protein
21
22 post-translational modifications.
23
24
25
26
27
28
29
30
31
32
33
34
35
36
37
38
39
40
41
42
43
44
45
46
47
48
49
50
51
52
53
54
55
56
57
58
59
60

1 ASSOCIATED CONTENT
2

3 **Supporting Information**
4

5 The following files are available free of charge:
6

7
8 Table S-1: Glycan compositions considered in database search; Table S-2: List of glycopeptides with
9 unusual sialyl structures, identified from human urinary glycoproteins; Table S-3: Additional glycan
10 structures deciphered from EThcD and HCD data manually; Figures S-1-29: EThcD data and the
11 corresponding HCD spectra for the glycopeptides listed in Table 1 and Table S-2; Figures S-30-35:
12 Supporting MS/MS data for the fucosyl glycoforms of Thr-346 of Protein YIPF3.
13
14
15
16
17
18
19
20
21

22 AUTHOR INFORMATION
23

24 **Corresponding Authors**
25

26 *Email: darula.zsuzsanna@brc.mta.hu, Tel/Fax: +36 62 599 773
27

28 *Email: medzihradzky.katalin@brc.mta.hu, Tel/Fax: +36 62 599 773
29
30
31
32

33 **Notes**
34

35 The authors declare no competing financial interest.
36
37
38
39

40 ACKNOWLEDGEMENTS
41

42 The authors wish to thank Robert Chalkley for his constructive comments on the discussion section, and
43 Kirk Hansen for correcting our Hunglish mistakes. We thank the MTA Cloud (<https://cloud.mta.hu/>) for
44 housing our Protein Prospector server. This work was supported by the following grants: New Szechenyi
45 Plan GOP-1.1.1-11-2012-0452, and the Economic Development and Innovation Operative Programmes
46 GINOP-2.3.2-15-2016-00001 and GINOP-2.3.2-15-2016-00020 from the Ministry for National Economy.
47
48
49
50
51
52
53
54
55
56
57
58
59
60

1 REFERENCES

- 2
3
4 (1) Varki, A.; Cummings, R. D.; Esko, J. D.; Stanley, P.; Hart, G. W.; Aebi, M.; Darvill, A. G.;
5
6 Kinoshita, T.; Packer, N. H.; Prestegard, J. H.; Schnaar, R. L.; Seeberger, P. H.; editors. *Essentials of*
7
8 *Glycobiology*. 3rd edition. Cold Spring Harbor (NY): Cold Spring Harbor Laboratory Press; 2015-
9
10 2017.
11
12
13
14
15 (2) Van den Steen, P.; Rudd, P. M.; Dwek, R. A.; Opdenakker, G. Concepts and principles of O-linked
16
17 glycosylation. *Crit. Rev. Biochem. Mol. Biol.* **1998**, *33*, 151- 8.
18
19
20
21
22 (3) Halim, A.; Brinkmalm, G.; Rüetschi, U.; Westman-Brinkmalm, A.; Portelius, E.; Zetterberg, H.;
23
24 Blennow, K.; Larson, G.; Nilsson, J. Site-specific characterization of threonine, serine, and tyrosine
25
26 glycosylations of amyloid precursor protein/amyloid beta-peptides in human cerebrospinal fluid.
27
28 *Proc. Natl. Acad. Sci. U S A.* **2011**, *108*, 11848-11853.
29
30
31
32
33 (4) Haslam, S. M.; North, S. J.; Dell, A. Mass spectrometric analysis of N- and O-glycosylation of
34
35 tissues and cells. *Curr. Opin. Struct. Biol.* **2006**, *16*, 584-591.
36
37
38
39
40 (5) Karlsson, H.; Larsson, J. M.; Thomsson, K. A.; Härd, I.; Bäckström, M.; Hansson G, C. High-
41
42 throughput and high-sensitivity nano-LC/MS and MS/MS for O-glycan profiling. *Methods Mol. Biol.*
43
44 **2009**, *534*, 117-131.
45
46
47
48
49 (6) Wada, Y.; Dell, A.; Haslam, S. M.; Tissot, B.; Canis, K.; Azadi, P.; Bäckström, M.; Costello, C. E.;
50
51 Hansson, G. C.; Hiki, Y.; Ishihara, M.; Ito, H.; Kakehi, K.; Karlsson, N.; Hayes, C. E.; Kato, K.;
52
53 Kawasaki, N.; Khoo, K. H.; Kobayashi, K.; Kolarich, D.; Kondo, A.; Lebrilla, C.; Nakano, M.;
54
55 Narimatsu, H.; Novak, J.; Novotny, M. V.; Ohno, E.; Packer, N. H.; Palaima, E.; Renfrow, M. B.;
56
57 Tajiri, M.; Thomsson, K. A.; Yagi, H.; Yu, S. Y.; Taniguchi, N. Comparison of methods for profiling
58
59
60

- 1 O-glycosylation: Human Proteome Organisation Human Disease Glycomics/Proteome Initiative
2
3
4 multi-institutional study of IgA1. *Mol. Cell. Proteomics* **2010**, *9*, 719-727.
5
6
7
- 8 (7) Zauner, G.; Kozak, R. P.; Gardner, R. A.; Fernandes, D. L.; Deelder, A. M.; Wührer, M. Protein O-
9 glycosylation analysis. *Biol. Chem.* **2012**, *393*, 687-708.
10
11
12
13
14
- 15 (8) Syka, J. E.; Coon, J. J.; Schroeder, M. J.; Shabanowitz, J.; Hunt, D. F. Peptide and protein sequence
16 analysis by electron transfer dissociation mass spectrometry. *Proc. Natl. Acad. Sci. U S A.* **2004**, *101*,
17 9528-9533.
18
19
20
21
22
23
- 24 (9) Frese, C. K.; Altelaar, A. F.; van den Toorn, H.; Nolting, D.; Griep-Raming, J.; Heck, A. J.;
25 Mohammed, S. Toward full peptide sequence coverage by dual fragmentation combining electron-
26 transfer and higher-energy collision dissociation tandem mass spectrometry. *Anal. Chem.* **2012**, *84*,
27 9668-9673.
28
29
30
31
32
33
34
35
- 36 (10) Darula, Z.; Medzihradszky, K. F. Analysis of Mammalian O-Glycopeptides-We Have Made a Good
37 Start, but There is a Long Way to Go. *Mol. Cell. Proteomics* **2018**, *17*, 2-17.
38
39
40
41
42
- 43 (11) Zhokhov, S. S.; Kovalyov, S. V.; Samgina, T. Y.; Lebedev, A. T. An EThcD-Based Method for
44 Discrimination of Leucine and Isoleucine Residues in Tryptic Peptides. *J. Am. Soc. Mass Spectrom.*
45 **2017**, *28*, 1600-1611.
46
47
48
49
50
51
- 52 (12) Pap, A.; Klement, E.; Hunyadi-Gulyas, E.; Darula, Z.; Medzihradszky, K. F. Status Report on the
53 High-Throughput Characterization of Complex Intact O-Glycopeptide Mixtures. *J. Am. Soc. Mass*
54 *Spectrom.* **2018**, doi: 10.1007/s13361-018-1945-7.
55
56
57
58
59
60

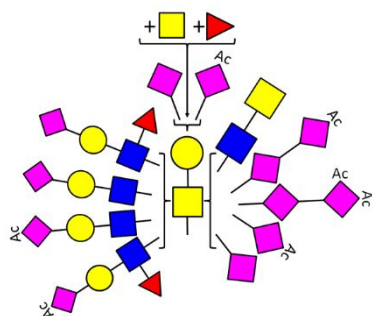
- 1 (13) Medzihradzky, K. F.; Kaasik, K.; Chalkley, R. J. Characterizing sialic acid variants at the
2 glycopeptide level. *Anal. Chem.* **2015**, *87*, 3064-3071.
3
4
5
6
7
8 (14) Baker, P. R.; Trinidad, J. C.; Chalkley, R. J. Modification site localization scoring integrated into a
9 search engine. *Mol. Cell. Proteomics* **2011**, doi: 10.1074/mcp.M111.008078.
10
11
12
13
14
15 (15) Halim, A.; Nilsson, J.; Rüetschi, U.; Hesse, C.; Larson, G. Human urinary glycoproteomics;
16 attachment site specific analysis of N- and O-linked glycosylations by CID and ECD. *Mol. Cell.*
17 *Proteomics* **2012**, *11*:M111.013649.
18
19
20
21
22
23
24 (16) Miura, Y.; Kato, K.; Takegawa, Y.; Kuroguchi, M.; Furukawa, J.; Shinohara, Y.; Nagahori, N.;
25 Amano, M.; Hinou, H.; Nishimura, S. Glycoblotting-assisted O-glycomics: ammonium carbamate
26 allows for highly efficient o-glycan release from glycoproteins. *Anal. Chem.* **2010**, *82*, 10021-10029.
27
28
29
30
31
32
33 (17) Takeuchi, M.; Amano, M.; Kitamura, H.; Tsukamoto, T.; Masumori, N.; Hirose, K.; Ohashi, T.;
34 Nishimura, S. I. N- and O-glycome analysis of serum and urine from bladder cancer patients using a
35 high-throughput glycoblotting method. *J. Glycomics Lipidomics* **2013**, *3*, 1-8.
36
37
38
39
40
41
42 (18) Trinidad, J. C.; Schoepfer, R.; Burlingame, A. L.; Medzihradzky, K. F. N- and O-glycosylation in
43 the murine synaptosome. *Mol. Cell. Proteomics* **2013**, *12*, 3474-3488.
44
45
46
47
48
49 (19) Medzihradzky, K. F.; Kaasik, K.; Chalkley, R. J. Tissue-Specific Glycosylation at the Glycopeptide
50 Level. *Mol. Cell. Proteomics* **2015**, *14*, 2103-2110.
51
52
53
54
55
56
57
58
59
60

- 1
2 (20) Chang, C. F.; Pan, J. F.; Lin, C. N.; Wu, I. L.; Wong, C. H.; Lin, C. H. Rapid characterization of
3
4 sugar-binding specificity by in-solution proximity binding with photosensitizers. *Glycobiology* **2011**,
5
6 *21*, 895–902.
7
8
9
- 10 (21) Domon, B.; Costello, C. E. A systematic nomenclature for carbohydrate fragmentations in FAB-
11
12 MS/MS spectra of glycoconjugates. *Glycoconjugate J.* **1988**, *5*, 397-409.
13
14
15
16
- 17 (22) Jin, C.; Kenny, D. T.; Skoog, E. C.; Padra, M.; Adamczyk, B.; Vitzeva, V.; Thorell, A.;
18
19 Venkatakrisnan, V.; Lindén, S. K.; Karlsson, N. G. Structural Diversity of Human Gastric Mucin
20
21 Glycans. *Mol. Cell. Proteomics* **2017**, *16*, 743-758.
22
23
24
25
- 26 (23) Wuhrer, M.; Deelder, A. M.; van der Burgt, Y. E. Mass spectrometric glycan rearrangements. *Mass*
27
28 *Spectrom Rev.* **2011**, *30*, 664-680.
29
30
31
32
- 33 (24) Wuhrer, M.; Balog, C. I.; Catalina, M. I.; Jones, F. M.; Schramm, G.; Haas, H.; Doenhoff, M. J.;
34
35 Dunne D. W.; Deelder, A. M.; Hokke, C. H. IPSE/alpha-1, a major secretory glycoprotein antigen
36
37 from schistosome eggs, expresses the Lewis X motif on core-difucosylated N-glycans. *FEBS J.*
38
39 **2006**, *273*, 2276-2292.
40
41
42
43
44
- 45 (25) Hashii, N.; Kawasaki, N.; Itoh, S.; Nakajima, Y.; Harazono, A.; Kawanishi, T.; Yamaguchi, T.
46
47 Identification of glycoproteins carrying a target glycan-motif by liquid chromatography/multiple-
48
49 stage mass spectrometry: identification of Lewis x-conjugated glycoproteins in mouse kidney. *J*
50
51 *Proteome Res.* **2009**, *8*, 3415-3429.
52
53
54
55
- 56 (26) Rossez, Y.; Maes, E.; Lefebvre Darroman, T.; Gosset, P.; Ecobichon, C.; Joncquel Chevalier Curt,
57
58 M.; Boneca, I. G.; Michalski, J. C.; Robbe-Masselot, C. Almost all human gastric mucin O-glycans
59
60

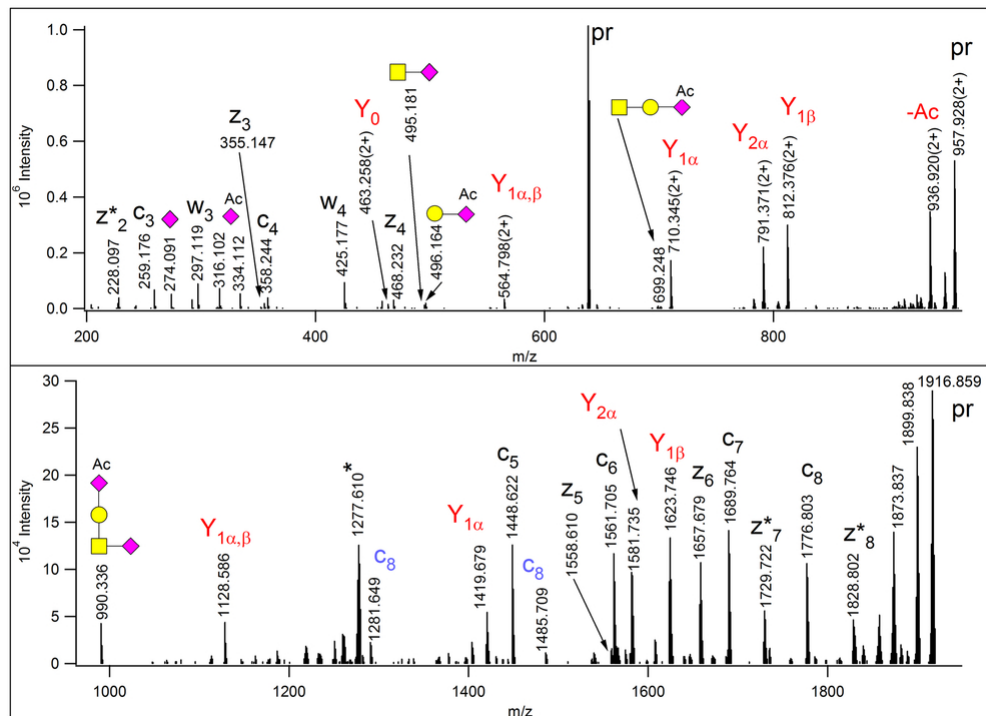
- 1 harbor blood group A, B or H antigens and are potential binding sites for *Helicobacter pylori*.
2
3
4 *Glycobiology*. **2012**, *22*, 1193-1206.
5
6
7
8 (27) Yabu, M.; Korekane, H.; Miyamoto, Y. Precise structural analysis of O-linked oligosaccharides in
9 human serum. *Glycobiology* **2014**, *24*, 542–553.
10
11
12
13
14
15 (28) Darula, Z.; Sherman, J.; Medzihradsky, K.F. How to dig deeper? Improved enrichment methods for
16 mucin core-1 type glycopeptides. *Mol. Cell. Proteomics* **2012**, doi: 10.1074/mcp.O111.016774.
17
18
19
20
21
22 (29) Sato, C.; Kitajima, K. Disialic, oligosialic and polysialic acids: distribution, functions and related
23 disease. *J. Biochem.* **2013**, *154*, 115-136.
24
25
26
27
28
29 (30) Hildebrandt, H; Dityatev, A. Polysialic Acid in Brain Development and Synaptic Plasticity. *Top.*
30 *Curr. Chem.* **2015**, *366*, 55-96.
31
32
33
34
35
36 (31) Martersteck, C. M.; Kedersha, N. L.; Drapp, D. A.; Tsui, T. G.; Colley, K. J. Unique alpha 2, 8-
37 polysialylated glycoproteins in breast cancer and leukemia cells. *Glycobiology* **1996**, *6*, 289-301.
38
39
40
41
42
43 (32) Kiang, W. L.; Krusius, T.; Finne, J.; Margolis, R. U.; Margolis, R. K. Glycoproteins and
44 proteoglycans of the chromaffin granule matrix. *J. Biol. Chem.* **1982** *257*, 1651-1659.
45
46
47
48
49
50 (33) Fukuda, M.; Lauffenburger, M.; Sasaki, H; Rogers, M. E.; Dell, A. Structures of novel sialylated O-
51 linked oligosaccharides isolated from human erythrocyte glycoporphins. *J. Biol. Chem.* **1987**, *262*,
52 11952-11957.
53
54
55
56
57
58
59
60

- 1
2 (34) Kitajima, K.; Sato, C.; Honda, N.; Matsuda, T.; Hara-Yokoyama, M.; Close, B.E.; and Colley, K.J.
3
4 Occurrence of alpha2,8-linked oligosialic acid residues in mammalian glycoproteins. In Inoue, Y.,
5
6 Lee, Y.C., and Troy, F.A. (eds), *Sialobiology and Other Novel Form of Glycosylation*, A
7
8 Monograph. Gakushin Syuppan, Osaka, Japan, **1999**, 69–76.
9
10
11
12
13 (35) Sato, C.; Yasukawa, Z.; Honda, N.; Matsuda, T.; Kitajima, K. Identification and adipocyte
14
15 differentiation-dependent expression of the unique disialic acid residue in an adipose tissue-specific
16
17 glycoprotein, adipo Q. *J. Biol. Chem.* **2001**, *276*, 28849-28856.
18
19
20
21
22 (36) Yasukawa, Z.; Sato, C.; Sano, K.; Ogawa, H.; Kitajima, K. Identification of disialic acid-containing
23
24 glycoproteins in mouse serum: a novel modification of immunoglobulin light chains, vitronectin, and
25
26 plasminogen. *Glycobiology* **2006**, *16*, 651-665.
27
28
29
30
31 (37) Takashima, S.; Ishida, H. K.; Inazu, T.; Ando, T.; Ishida, H.; Kiso, M.; Tsuji, S.; Tsujimoto, M.
32
33 Molecular cloning and expression of a sixth type of alpha 2,8-sialyltransferase (ST8Sia VI) that
34
35 sialylates O-glycans. *J. Biol. Chem.* **2002**, *277*, 24030-24080.
36
37
38
39
40 (38) Teinturier-Lelièvre, M.; Julien, S.; Juliant, S.; Guerardel, Y.; Duonor-Cérutti, M.; Delannoy, P.;
41
42 Harduin-Lepers, A. Molecular cloning and expression of a human hST8Sia VI (alpha2,8-
43
44 sialyltransferase) responsible for the synthesis of the diSia motif on O-glycosylproteins. *Biochem. J.*
45
46 **2005**, *392*, 665-674.
47
48
49
50
51 (39) Klein, A.; Roussel, P. O-acetylation of sialic acids. *Biochimie* **1998**, *80*, 49-57.
52
53
54
55
56
57
58
59
60

- 1 (40) Argüeso, P.; Sumiyoshi, M. Characterization of a carbohydrate epitope defined by the monoclonal
2 antibody H185: sialic acid O-acetylation on epithelial cell-surface mucins. *Glycobiology* **2006**, *16*,
3 1219-1228.
4
5
6
7
8
9
10 (41) Sen, G.; Chowdhury, M.; Mandal, C. O-acetylated sialic acid as a distinct marker for differentiation
11 between several leukemia erythrocytes. *Mol. Cell. Biochem.* **1994**, *136*, 65-70.
12
13
14
15
16
17
18
19
20
21
22
23
24
25
26
27
28
29
30
31
32
33
34
35
36
37
38
39
40
41
42
43
44
45
46
47
48
49
50
51
52
53
54
55
56
57
58
59
60

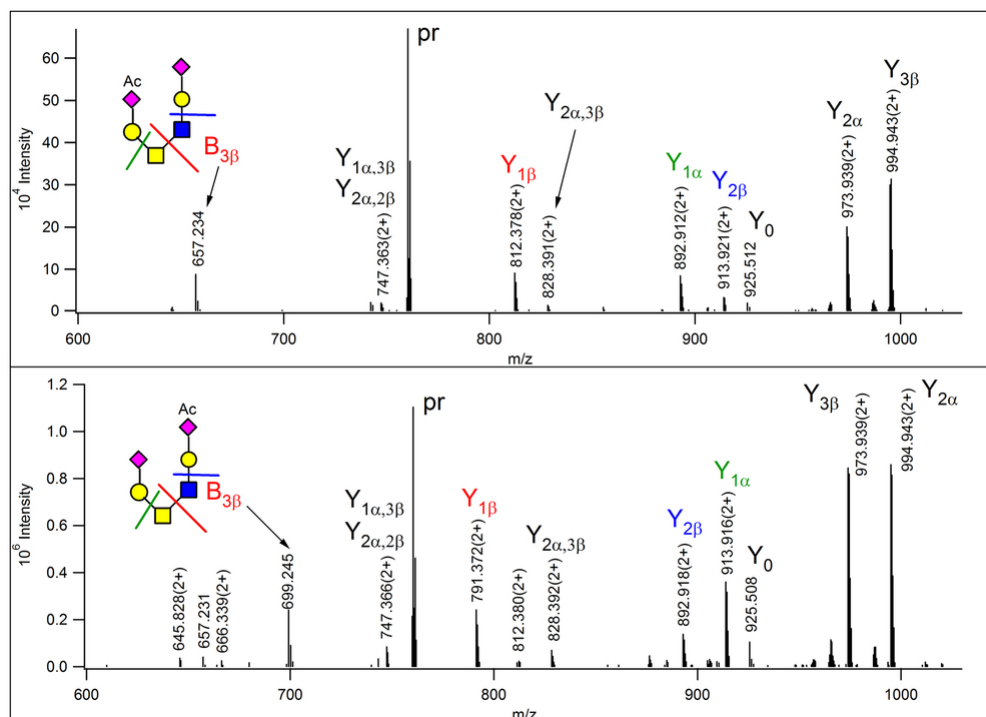


For TOC only



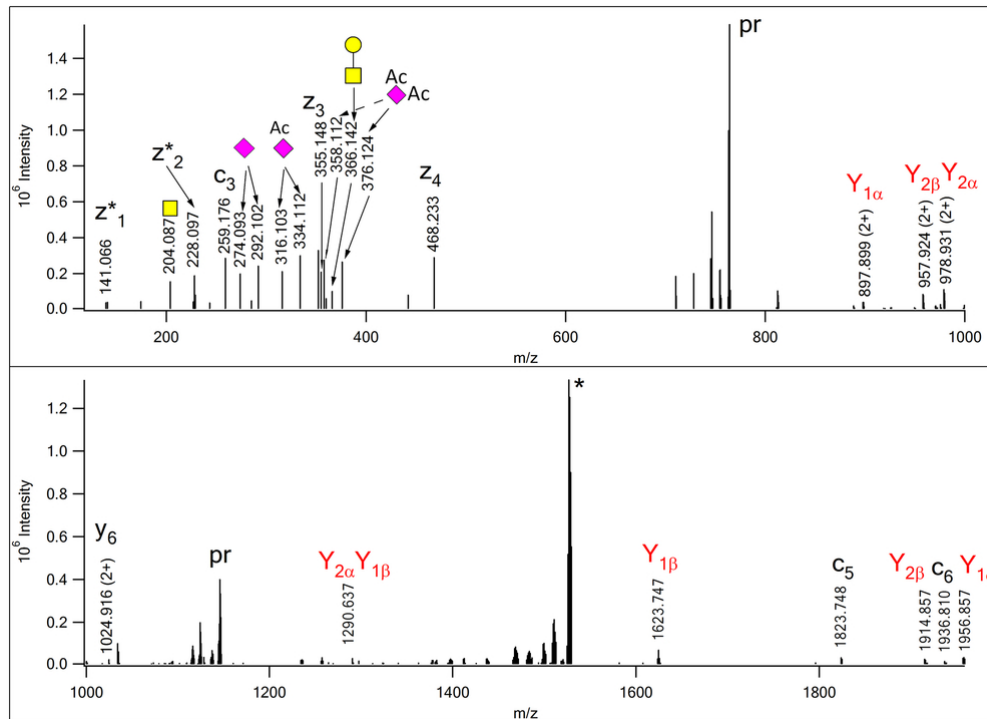
ETHcD spectrum of m/z 638.954(3+), identified as 342AVAVT(HexNAcHexNeuAcNeuAcAc)LQSH350 of Protein YIPF3. The Gal of the mucin-type core 1 structure is capped with a Neu5,9Ac2 moiety. (This sugar is listed as NeuAcAc in the glycan library for database searches). Oxonium and related ions are labeled according to the CFG recommendations, for the reducing end fragments – printed in red - the Domon-Costello nomenclature is followed²¹. The sialic acid loss from the core GalNAc yields the Y1 β fragment. z+1 peptide ions are distinguished with asterisks. Peptide fragments in blue indicate that some glycan fragmentation occurred in ETHcD, the loss of the NeuAc and GalNeu5,9Ac2 from the c8 fragment, respectively. The asterisk-labeled ion is the charge-reduced form of a doubly charged coeluting molecule.

84x61mm (300 x 300 DPI)



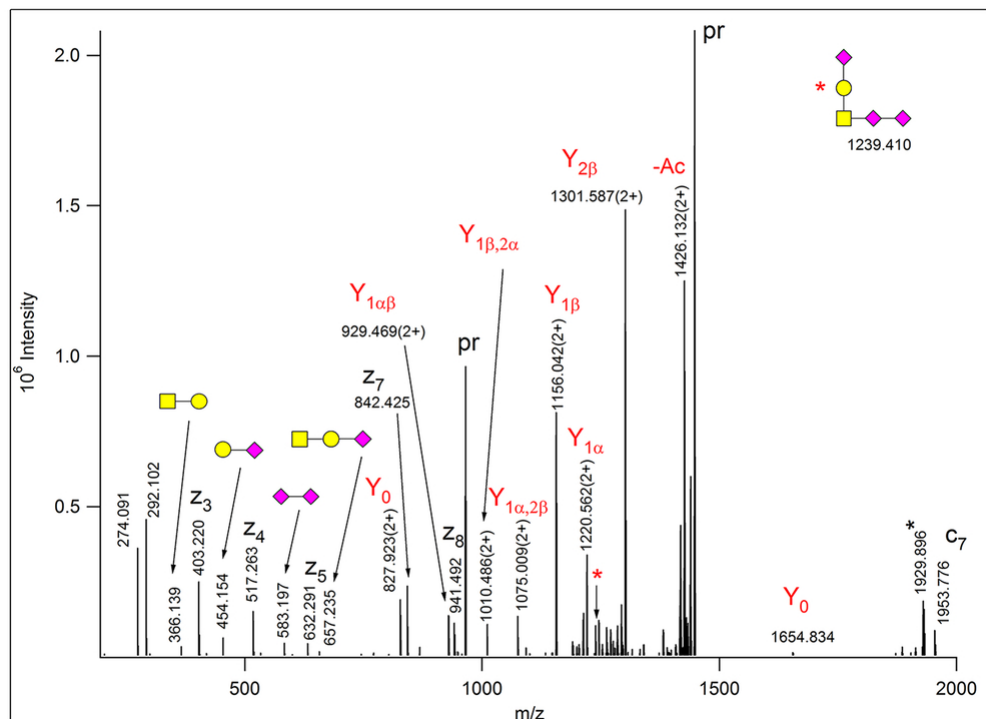
Part of the ETHcD spectra acquired from m/z 760.664(3+) at $RT=14.95$ min (Lower panel) and at $RT=18.29$ min (Upper panel). Both spectra were assigned as 342AVAVT(HexNAc2Hex2NeuAcNeuAcAc)LQSH350 of Protein YIPF3 (for full spectra see Figures S-7 & S-8). (NeuAcAc stands for Neu5,9Ac2 in the glycan library for database searches.) However, the glycan fragments revealed isomeric glycoforms. The diagnostic fragment ions and the underlying cleavages are indicated in matching colors.

84x61mm (300 x 300 DPI)



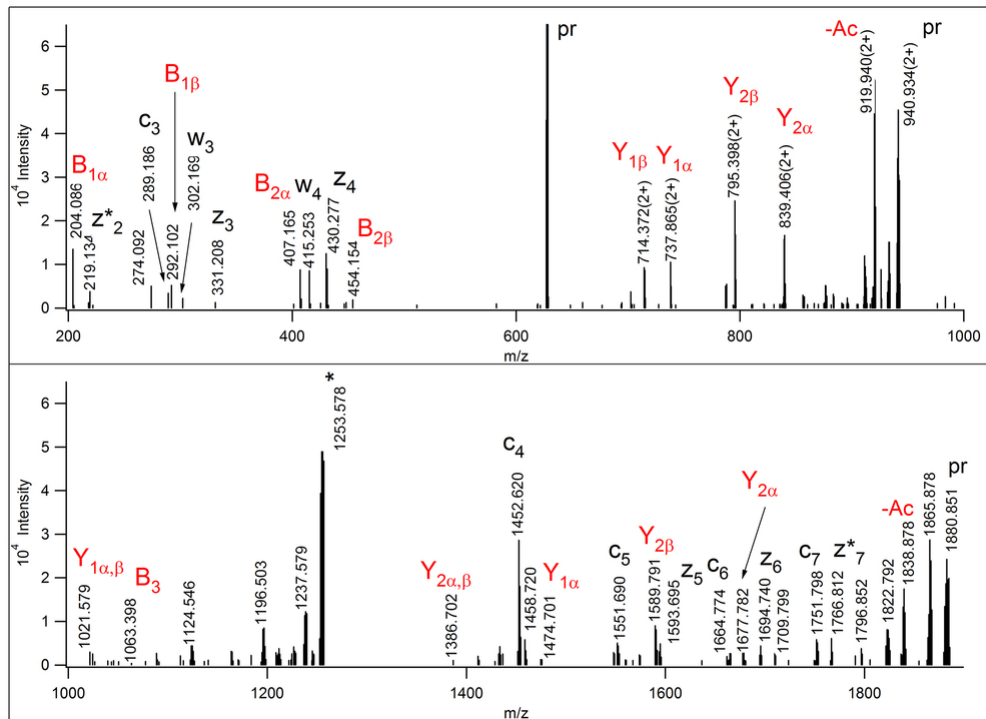
EThcD spectrum of m/z 763.992(3+) manually assigned as 342AVAVTLQSH350, modified at Thr-346 with a core 1 glycan that features a Neu5,9Ac2 on the Gal residue, and a NeuAc-Neu4,5,9Ac3 disialo-unit on the core GalNAc. 'Pr' indicates the different forms of the precursor ion. z+1 peptide fragments are distinguished with asterisks. The oxonium ions identifying the three different sialic acids are labeled with the CFG symbols, for the reducing end fragments - printed in red - the Domon-Costello nomenclature is followed²¹. The GalNAc modifications were considered the β -arm. The asterisk-labeled ion is the charge-reduced form of a doubly charged coeluting molecule.

84x61mm (300 x 300 DPI)



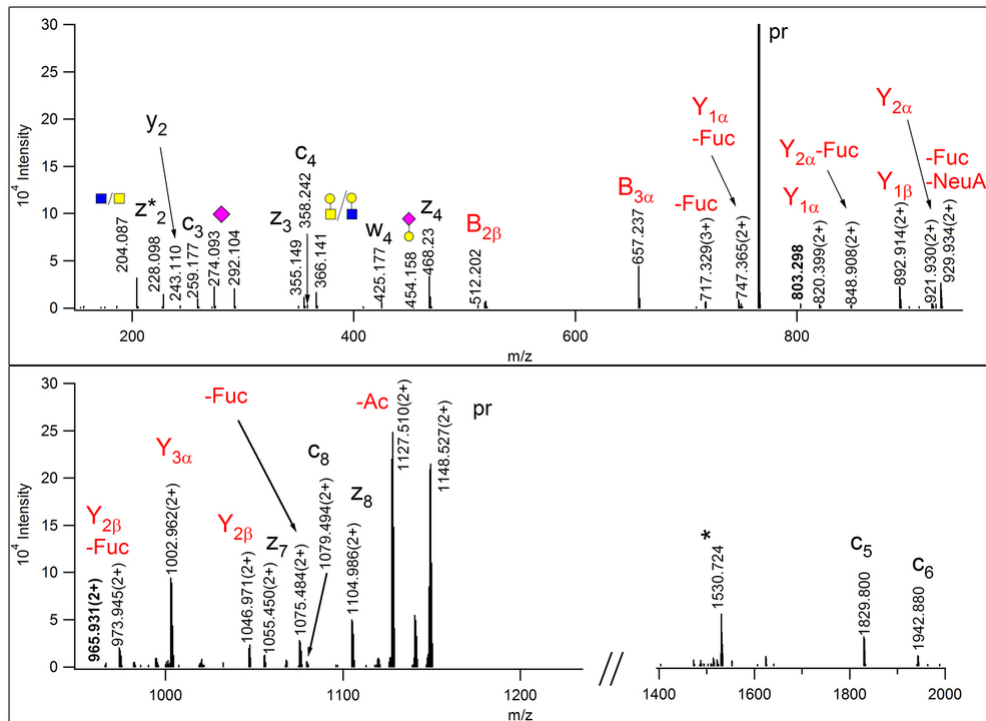
ETcD spectrum of m/z 965.092(3+), identified as 93DVSTPPT(HexNAcHexNeuAc3)VLPDNFPR107 of Insulin-like growth factor II. The precursor ion and its charge-reduced form are labeled with 'pr'. The nonreducing end fragments are labeled with cartoons according to the CFG recommendations, the reducing end fragments, printed in red, follow the nomenclature²¹. The inset shows the intact glycan and its oxonium ion is labeled by a red asterisk. The other asterisk-labeled ion is the charge-reduced form of a doubly charged coeluting molecule. For full peaklist see Figure S-10.

84x61mm (300 x 300 DPI)



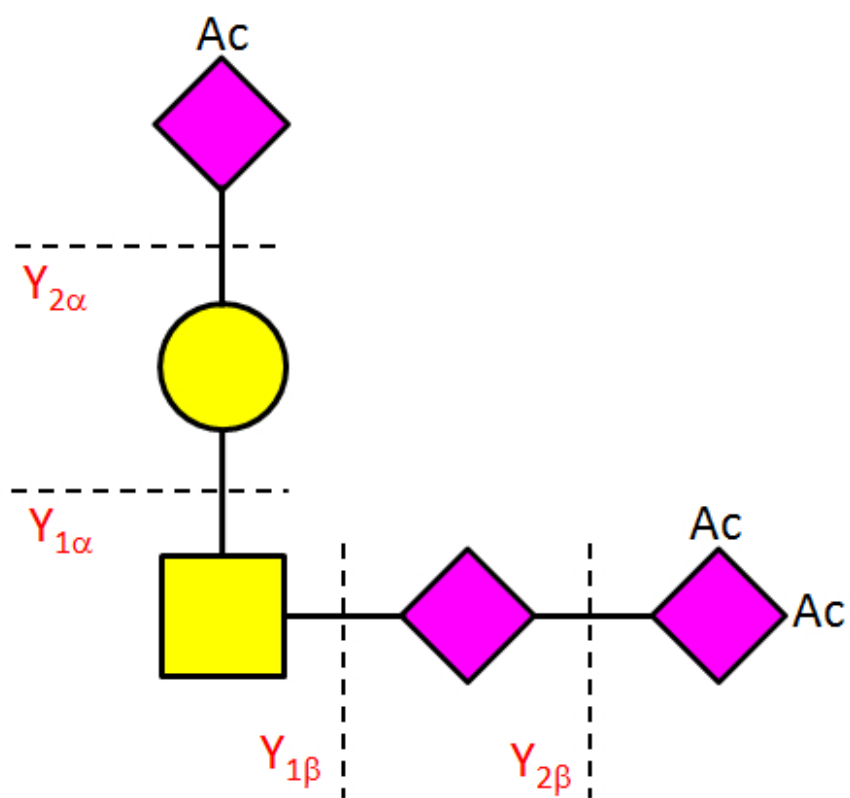
EThcD spectrum of m/z 627.634(3+). The database search permitting unspecified modifications identified as 45VATT(1062.388)VISK52 of Plasma protease C1 inhibitor. z^* indicates a $z+1$ peptide fragment. The intact glycan oxonium ion confirms that the peptide is modified by a single oligosaccharide of HexNAc3HexNeuAc composition. The glycan fragments helped to decipher the branching and linkages within the oligosaccharide, a core 2 based LacdiNAc-like structure²². Scheme 2 illustrates which bonds are cleaved. z^* indicates a $z+1$ peptide fragment. The asterisk-labeled ion is the charge-reduced form of a doubly charged coeluting molecule.

84x61mm (300 x 300 DPI)



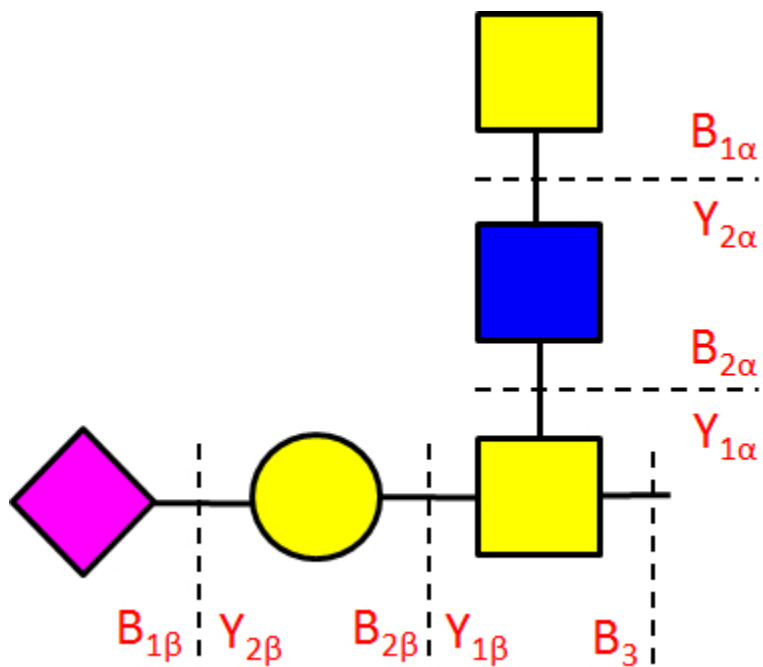
ETHcD spectrum of m/z 766.008(3+) that was manually assigned as 342AVAVTLQSH350 of Protein YIPF3 bearing a HexNAc3Hex2FucNeuAc glycan on Thr-346. The precursor ion and its charge-reduced form are labeled with 'pr'; the charge-reduced form of a coeluting doubly charged component is indicated with an asterisk. The glycan is assigned as a core 2 glycan featuring the A antigen linked to the GalNAc. A similar core 2 A antigen has been described on gastric mucin by Rossez et al.26 Scheme 4 illustrates which bonds are cleaved. m/z values printed in bold label fragments that indicate fucose transfer between the antennae: m/z 803.298 represents a HexNAcHexFucNeuAc structure, while m/z 965.931(2+) was formed via HexNAcHex loss from the precursor ion.

84x61mm (300 x 300 DPI)



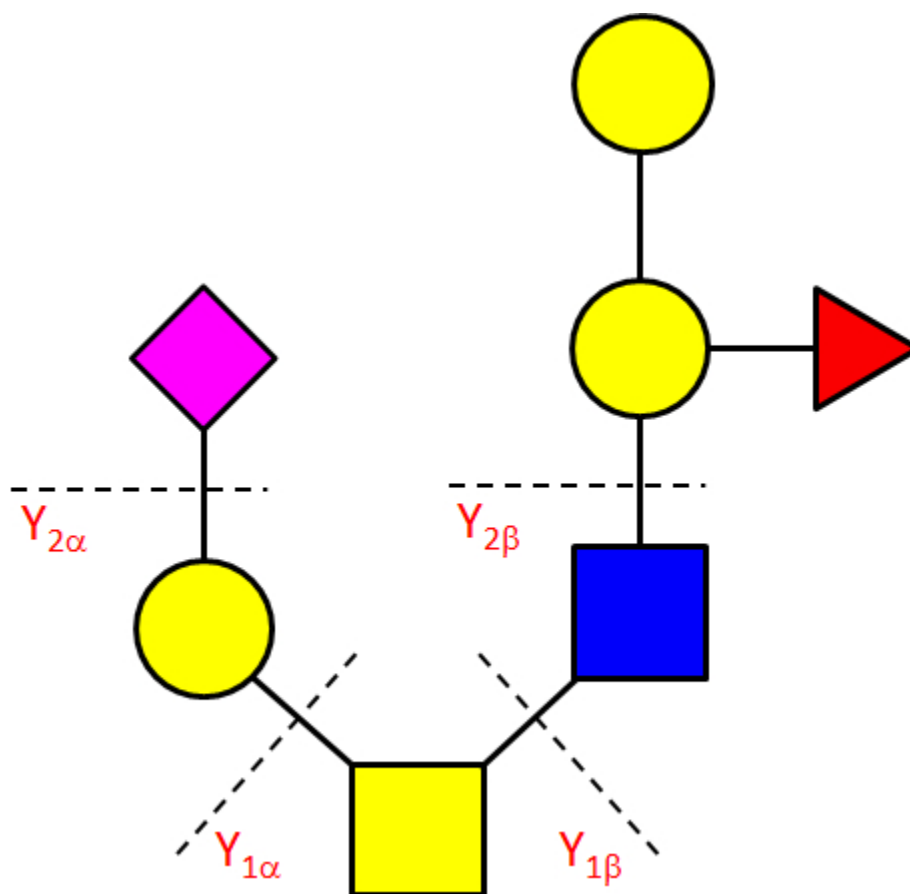
Fragmentation of the glycan structure assigned from the spectrum in Figure 3.

136x114mm (96 x 96 DPI)



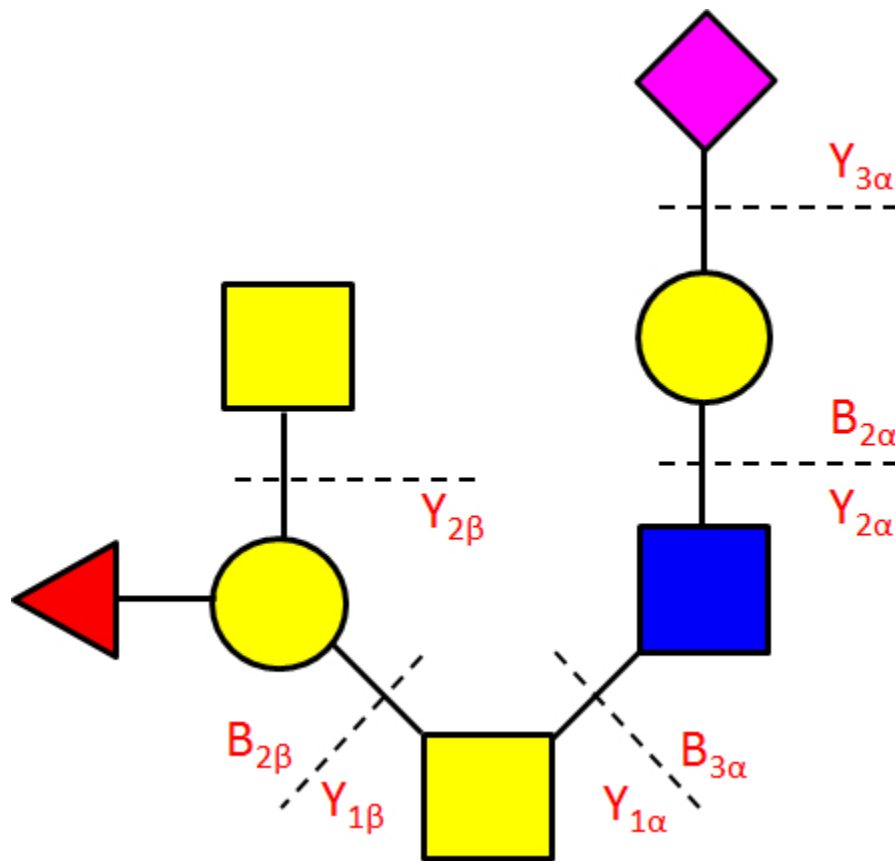
Fragmentation of the glycan structure assigned from the spectrum in Figure 5.

103x91mm (96 x 96 DPI)



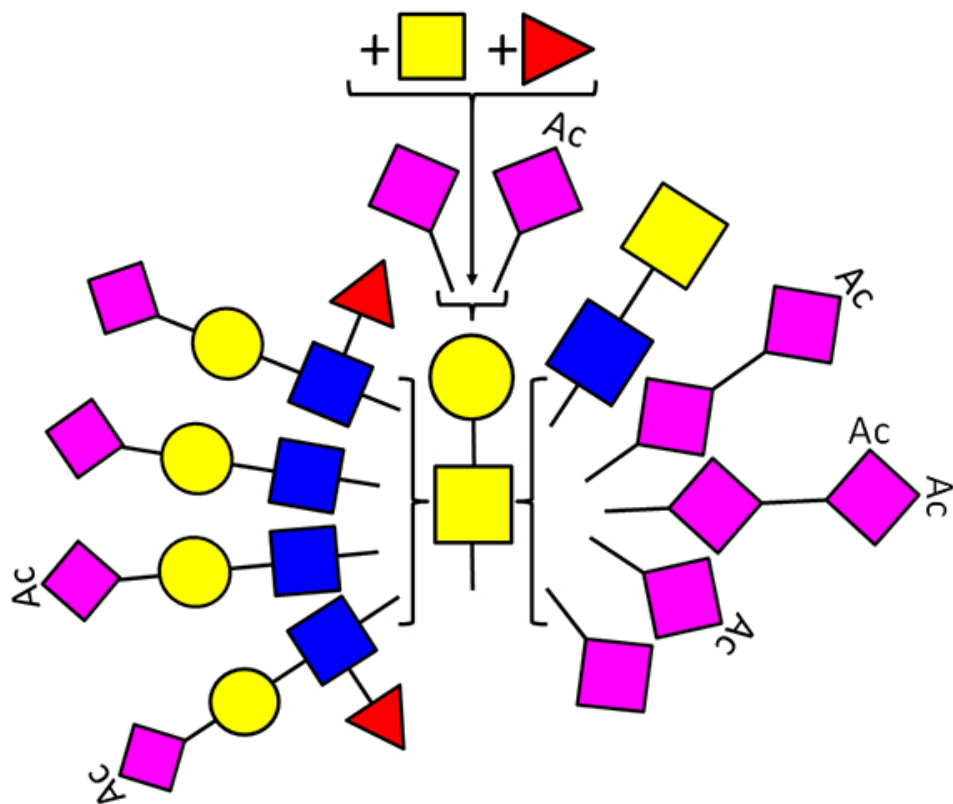
Fragmentation of the mucin core 2 glycan carrying blood-type antigen B structure assigned from the spectrum in Figure 6.

124x118mm (96 x 96 DPI)



Fragmentation of the glycan structure assigned from the spectrum in Figure 7.

125x114mm (96 x 96 DPI)



50x43mm (300 x 300 DPI)